Biogeosciences Discuss., 9, 10669–10724, 2012
www.biogeosciences-discuss.net/9/10669/2012/
doi:10.5194/bgd-9-10669-2012

Biogeosciences Discussions

Atlantic and Arctic sea-air CO_2 fluxes, 1990–2009

U. Schuster[1], G. A. McKinley[2], N. Bates[3], F. Chevallier[4], S. C. Doney[5], A. R. Fay[2], M. González-Dávila[6], N. Gruber[7], S. Jones[1,8], J. Krijnen[1,8], P. Landschützer[1,8], N. Lefèvre[9], M. Manizza[10], J. Mathis[11], N. Metzl[12], A. Olsen[13], A. F. Rios[14], C. Rödenbeck[15], J. M. Santana-Casiano[6], T. Takahashi[16], R. Wanninkhof[17], and A. J. Watson[1]

[1]University of East Anglia, Norwich, UK
[2]University of Wisconsin, Madison, WI, USA
[3]Bermuda Institute of Ocean Science, Bermuda
[4]LSCE-IPSL, Paris, France
[5]Woods Hole Oceanographic Institution, Woods Hole, MA, USA
[6]Universidad de Las Palmas de Gran Canaria, Las Palmas, Gran Canaria
[7]ETH-Zürich, Zürich, Switzerland
[8]University of East Anglia, Norwich, UK
[9]LOCEAN, Université Pierre et Marie Curie, Paris, France
[10]Scripps Institution of Oceanography, La Jolla, CA, USA
[11]University of Alaska-Fairbanks, Fairbanks, AK, USA
[12]LOCEAN-IPSL, CNRS, UPMC, Paris, France
[13]Uni Research, Bergen, Norway

[14]Instituto de Investigaciones Marinas, IIM-CSIC, Vigo, Spain
[15]Max-Planck-Institut für Biogeochemie, Jena, Germany
[16]Lamont Doherty Earth Observatory of Columbia University, Palisades, NY, USA
[17]NOAA/Atlantic Oceanographic and Meteorological Laboratory, Miami, FL, USA

Received: 25 June 2012 – Accepted: 28 June 2012 – Published: 9 August 2012

Correspondence to: U. Schuster (u.schuster@uea.ac.uk)

Published by Copernicus Publications on behalf of the European Geosciences Union.

BGD
9, 10669–10724, 2012

Abstract

The Atlantic and Arctic oceans are critical components of the global carbon cycle. Here we quantify the net sea-air CO_2 flux, for the first time, across different methodologies for consistent time and space scales, for the Atlantic and Arctic basins. We present the long-term mean, seasonal cycle, interannual variability and trends in sea-air CO_2 flux for the period 1990 to 2009, and assign an uncertainty to each. We use regional cuts from global observations and modelling products, specifically a pCO_2-based CO_2 flux climatology, flux estimates from the inversion of oceanic and atmospheric data, and results from six ocean biogeochemical models. Additionally, we use basin-wide flux estimates from surface ocean pCO_2 observations based on two distinct methodologies. Our best estimate of the contemporary sea-to-air flux of CO_2 (sum of anthropogenic and natural components) by the Atlantic between 40° S and 79° N is $-0.49 \pm 0.11\,\mathrm{Pg\,C\,yr^{-1}}$ and by the Arctic is $-0.12 \pm 0.06\,\mathrm{Pg\,C\,yr^{-1}}$, leading to a combined sea-to-air flux of $-0.61 \pm 0.12\,\mathrm{Pg\,C\,yr^{-1}}$ for the two decades (negative reflects ocean uptake). We do find broad agreement amongst methodologies with respect to the seasonal cycle in the subtropics of both hemispheres, but not elsewhere. Agreement with respect to detailed signals of interannual variability is poor; and correlations to the North Atlantic Oscillation are weaker in the North Atlantic and Arctic than in the equatorial region and South Subtropics. Linear trends for 1995 to 2009 indicate increased uptake and generally correspond between methodologies in the North Atlantic, but there is disagreement amongst methodologies in the equatorial region and South Subtropics.

1 Introduction

The ocean is the dominant removal pathway of anthropogenic CO_2 from the atmosphere on centennial timescales (Sabine et al., 2004; Khatiwala et al., 2009). Estimates for the present-day, global ocean anthropogenic CO_2 sink have converged to

BGD
9, 10669–10724, 2012

−1.9 to −2.4 $PgC\,yr^{-1}$ (Wanninkhof et al., 2012), the same magnitude as the mean net global CO_2 sink in the terrestrial biosphere. Contemporary net sea-air CO_2 fluxes reflect a combination of natural processes and anthropogenic CO_2 uptake, and spatially-integrated CO_2 fluxes at ocean basin scales provide important metrics of the ocean carbon cycle and anthropogenic CO_2 transient (Gruber et al., 2009; Takahashi et al., 2009). The current best-estimate for the global contemporary sink is $-1.7\,PgC\,yr^{-1}$ (Gruber et al., 2009), with the difference between this and the anthropogenic primarily being a natural outgassing of carbon input by rivers ($0.45\,PgC\,yr^{-1}$, Jacobson et al., 2007).

In this manuscript, a contribution to the Regional Carbon Cycle Assessment Project (RECCAP, Canadell et al., 2011), we review the state of our understanding of contemporary carbon fluxes between the atmosphere and ocean for the Arctic and Atlantic. Previous work has indicated that the net annual sea-air CO_2 flux for the Arctic and Atlantic is negative (into the ocean). Modeling studies and ocean inversions have suggested that nearly all of this net flux is driven by the uptake of anthropogenic CO_2 (Gruber et al., 2009). The tropical region is an annual mean source of CO_2 to the atmosphere, whilst the mid- and high-latitudes are annual mean sinks of CO_2. The few CO_2 flux estimates existing for the Arctic concur that the region is an annual mean sink.

At the global scale, inter-annual variability (IAV) in sea-air flux has been well-established to be dominated globally by the El Niño/Southern Oscillation (ENSO) cycle (Peylin et al., 2005; McKinley et al., 2004a, b; Feely et al., 2006; Ishii et al., 2009) whilst the impact of variations in the dominant mode of North Atlantic variability, i.e., the North Atlantic Oscillation, has remained difficult to quantify (Gruber et al., 2009; McKinley et al., 2004; Peylin et al., 2005; Thomas et al., 2008). Trends in ocean carbon uptake have become of significant interest in recent years because of a concern that climate-driven feedbacks may be limiting ocean carbon uptake (Canadell et al., 2011; Le Quéré et al., 2009, 2010; Schuster et al., 2009; McKinley et al., 2011; Lovenduski et al., 2008). In this study, we review in detail these previous results with respect to

BGD
9, 10669–10724, 2012

mean CO_2 uptake, its interannual variability, and its recent trends for 5 key sub-regions of the Arctic and Atlantic.

1.1 The Arctic

The Arctic Ocean is a complex region of sea-air CO_2 fluxes, due to its unique characteristics. Its biogeochemical cycle is dominated by its lateral inputs, including nutrient-rich inputs through the Barents Sea (North Atlantic) and Chukchi Sea (North Pacific), which lead to high biological production and consequent under-saturation of surface CO_2 (Omar et al., 2007), and carbon-saturated riverine (Anderson et al., 2009) and meltwater inputs from the surrounding land masses. These inputs have a disproportionate effect on the Arctic Ocean as it encompasses only 3 % of the global ocean's total area, but received ~ 10 % of total global runoff. A significant proportion (53 %) of the Arctic basin consists of continental shelf margins, whose inorganic and organic carbon content is highly variable and notoriously difficult to assess. Finally, much of the ocean is covered by seasonal sea ice, which restricts carbon fluxes in winter, while high rates of primary production over inflow shelves lead to under-saturated open water in summer months (e.g. Bates, 2006).

The dynamics of the Arctic Ocean make estimates of the sea-air CO_2 flux very difficult, with large uncertainties. However, it is generally agreed that the ocean as a whole is a year-round CO_2 sink (Bates and Mathis, 2009 and references therein), with high seasonal variability due to the sea-ice cycle and related biological activity (Bates, 2006; Kaltin and Anderson, 2005). For example, there are areas of the Arctic Ocean such as the Chukchi Sea and Barents Sea where there is large CO_2 uptake per unit area (e.g. Omar et al., 2007; Bates, 2006) due to very high rates of summertime pelagic phytoplankton primary production. Early assessments of the rate of sea-air CO_2 exchange in the Arctic Ocean using indirect mass balance approaches suggested that the integrated net sea-air CO_2 flux for the entire Arctic Ocean was in the range of −0.024 to $-0.129\,\mathrm{Pg\,C\,yr^{-1}}$ (Anderson et al., 1990, 1994). A more recent review of available sea-air CO_2 flux and supporting seawater carbonate chemistry data gave a range of

BGD
9, 10669–10724, 2012

−0.06 to −0.199 Pg C yr^{-1} for the Arctic Ocean (Bates and Mathis, 2009). Such studies used a scaling-up approach where relatively sparse and often very localized data were translated into estimates for each region of the Arctic Ocean. A more recent estimate of CO_2 fluxes (Arrigo et al., 2010) indicated a flux of −0.118 Pg C yr^{-1} for the period 1998–2003. A model study of the carbon cycle of the Arctic (Manizza et al., 2011), estimates the flux of CO_2 for the Arctic Ocean north of 65° N to be −0.059 Pg C yr^{-1}. This estimate comes from an ocean carbon cycle model embedded in high-resolution ocean circulation model of the Arctic Ocean with applied re-analyzed forcing corresponding to the 1992 to 2001 period. For the Siberian Sea, Anderson et al. (2009) state an outgassing of +0.010 Pg C yr^{-1}, which is higher than any of the Bates and Mathis (2009) quoted values, which range −0.0059 to +0.0003 Pg C yr^{-1}, which brings down the high end of that estimate for the net sea-air flux from −0.199 to approximately −0.175 Pg C yr^{-1}. Based on these reported values, the long-term mean Arctic Ocean sea-air CO_2 flux is −0.06 to −0.18 Pg C yr^{-1}, or −0.12 ± 0.06 Pg C yr^{-1}.

There is insufficient data available to provide a quantitative assessment of interannual variability or long-term trends in CO_2 flux in the Arctic, although the dynamic nature of the region suggests that the former would be relatively large. Speculation over the future trend of the carbon flux in this region has suggested that the net CO_2 sea-air flux in the Arctic will grow more strongly negative associated with further sea-ice loss. It is important to note that previous synthesis and model studies of the Arctic Ocean CO_2 flux were based on data collected prior to the major summertime sea-ice loss event in 2007 (Bates and Mathis, 2009); a transformation in the sea-ice extent of the Arctic that has continued to the present day. More recent surveys conducted suggest that there may not be an increase in CO_2 uptake since the 2007 sea-ice loss event (Cai et al., 2010). Thus estimates of the current Arctic Ocean CO_2 flux remain highly uncertain given that there are competing processes either reducing or increasing the rate of sea-air CO_2 transfer (e.g. Bates and Mathis, 2009). Processes acting to reduce the CO_2 flux into the ocean include warming, increased sea-ice melt and freshwater contributions of the polar mixed layer, and enhanced riverine discharge of dissolved organic

BGD
9, 10669–10724, 2012

carbon and subsequent remineralization to CO_2. In contrast, greater areal extent of summertime sea-ice free open water, increase in pelagic phytoplankton primary production (e.g. Arrigo et al., 2008) and translocation of marine ecosystems in responses to changes in sea-ice act oppositely to potentially increase CO_2 uptake. Complicating future assessment of the trajectory of the Arctic Ocean CO_2 flux is the loss of multiyear sea-ice and replacement by thinner first-year sea-ice that has implications for winter sea-air CO_2 transfer across sea-ice. Similarly, changing optical regimes below thinning sea-ice may also significantly change rates of pelagic phytoplankton primary production (Arrigo et al., 2012) and uptake of CO_2 on the polar shelves and sea-ice retreat zones of the Arctic.

1.2 The subpolar North Atlantic

The subpolar North Atlantic, between 50° N and 80° N, is a strong sink for atmospheric CO_2. Takahashi et al. (2009) estimated it at $-0.27\,Pg\,C\,yr^{-1}$, equivalent to 15 % of the total global oceanic CO_2 uptake. This strong sink is a result of a sizeable natural CO_2 sink, being roughly doubled by the uptake of anthropogenic CO_2 (Gruber et al., 2009). In fact, this area constitutes one of the most intense anthropogenic CO_2 sinks per unit area (Mikaloff Fletcher et al., 2006). Coupled physical-biogeochemical models indicate an sea-air flux variability of approximately $0.1\,Pg\,C\,yr^{-1}$, and illustrate that the opposing effects of variability in sea-surface temperature (SST), convective fluxes, and biology dampen the sea-air flux variability (Le Quéré et al., 2000; McKinley et al., 2004; Thomas et al., 2008; Ullman et al., 2009; Bennington et al., 2009).

In recent years, observational studies have suggested that the net CO_2 flux into the ocean has declined in the subpolar North Atlantic, weakening by about 50 % in the south-eastern part of the subpolar gyre, from $-0.20\,Pg\,C\,yr^{-1}$ in the mid 1990s to $-0.09\,Pg\,C\,yr^{-1}$ in the mid 2000s (Schuster et al., 2009). Across the subpolar region, a summer rise in the partial pressure of sea surface CO_2 (pCO_2) was identified as between 2.3 and $3.5\,\mu atm\,yr^{-1}$ between 1982 and 1998, whilst the atmospheric CO_2 rise

BGD
9, 10669–10724, 2012

over the same time period was 1.5 µatm yr^{-1} (Lefevre et al., 2004). Furthermore, between winters of 2001 and 2008, an even faster rise of surface water pCO_2 of the order of 5.8 ± 1.1 µatm yr^{-1} and 7.2 ± 1.3 µatm yr^{-1} was reported (Metzl et al., 2010). These studies identified a decrease of the ocean-atmosphere pCO_2 difference (ΔpCO_2), suggesting a decrease in the carbon sink, as has also been highlighted in other studies (Corbière et al., 2007; Omar and Olsen, 2006; Olsen et al., 2006).

However, coupled physical-biogeochemical models and atmospheric inversions do not suggest a declining sink in the subpolar gyre from the mid-1990s to the mid-2000s. An atmospheric inversion study (Rödenbeck, 2005) tentatively suggested an increase in CO_2 uptake between 50° N and 80° N of 0.03 Pg C yr^{-1} (0.15 to 0.18 Pg C yr^{-1}) during this time. A regional physical-biogeochemical model (Ullman et al., 2009), identified a similar increase of 0.04 Pg C yr^{-1} (0.22 to 0.26 Pg C yr^{-1}) in the carbon uptake over the same period and same region, with the first-order mechanism being reduced convective supply of dissolved inorganic carbon (DIC) from depth. Thomas et al. (2008) find a slight decrease in the CO_2 uptake by the ocean in the eastern subpolar gyre from 1996 to 2004, due to a surface ocean pCO_2 increase slightly exceeding the atmospheric CO_2 growth rate of 1.6 ppm yr^{-1}. Thomas et al. (2008) attribute this to a decrease in horizontal advection of low DIC waters from the subtropics between 1997 and 2004, and they note that recent trends are primarily driven by decadal timescale climate variability.

Comparison of these studies suggesting declines in carbon uptake is difficult because of their lack of coherence in time and space. For example, the observations are sparse and tend to be concentrated along shipping lanes where Volunteer Observing Ships (VOS) operate; and models are coarse in spatial resolution and crudely parameterize critical biological processes. Further, it is critical to distinguish whether the significant decadal climate variability in this region is responsible for observed changes, as opposed to long-term trends. McKinley et al. (2011) addressed these issues by using an updated pCO_2 database (Takahashi et al., 2009) to estimate pCO_2 trends in 3 North Atlantic basin-scale biomes for a range of timeframes between 1981 and 2009.

BGD
9, 10669–10724, 2012

They illustrated that in the subpolar region it takes at least 25 yr for the driving force for ocean carbon uptake to be predominantly anthropogenic carbon accumulation in the atmosphere; and the shorter-term changes reported from observations are best interpreted as the result of decadal variability and not by long-term declines in ocean carbon sequestration (e.g. Gruber et al., 2009).

Variability in the subpolar carbon sink is due to the various and opposing influences of the decadal climate variability, with the North Atlantic Oscillation (NAO) is the dominant mode of climate variability here. A negative NAO phase is characterized by less extreme wind events in winter in the subpolar gyre (Marshall et al., 2001). A shift from a positive to negative NAO during the mid-1990s to the mid-2000s resulted in increased pCO_2 in this region, primarily caused by warmer surface waters in the subpolar gyre (Corbière et al., 2007). Additionally, the strength of the subpolar gyre circulation decreased in the 1990s (Hakkinen and Rhines, 2009), allowing the advection of warmer waters to penetrate the subpolar region and reducing the CO_2 uptake here (Schuster and Watson, 2007). However, at the same time, the decline in the NAO led to reduced convective mixing of high DIC waters from depth, and this lowered pCO_2 and promoted increased carbon uptake (Ullman et al., 2009). A reduction in biological activity is another factor that could explain change in CO_2 uptake (Lefevre et al., 2004). However, the NAO explains only about 30 % of the climate variability (Marshall et al., 2001). Metzl et al. (2010) attribute a fast rise of surface water pCO_2 observed in the early 2000s to seawater carbonate chemistry changes that are unlikely to be caused by NAO variability. Whether NAO-driven or not, the fact that the CO_2 sink is influenced by these multiple, vigorous and opposing mechanisms makes a precise determination challenging, and makes elucidation of effects, particularly as they vary on interannual to decadal timescales, prone to both observational and model uncertainty.

1.3 The Subtropical North Atlantic

The subtropical and temperate North Atlantic from 14° N to 50° N is a significant sink for atmospheric CO_2, with an estimated net sea-air CO_2 flux of $-0.22\,\mathrm{Pg\,C\,yr^{-1}}$ in 2000

BGD
9, 10669–10724, 2012

(Takahashi et al., 2009). Similar to the subpolar North Atlantic, this large flux is interpreted to be a consequence of a superposition of a large uptake of anthropogenic CO_2 with a large sink of natural CO_2, with the latter driven by a net heat loss and an efficient biological pump (Gruber et al., 2009). The trends and year-to-year variations in these net sea-air fluxes have been observed both in the Western Subtropical Atlantic at the Bermuda Atlantic Time Series (BATS, e.g. Bates, 2007), and in the Eastern Subtropical Atlantic at European Station for Time Series in the Ocean (ESTOC, e.g. González-Dávila et al., 2007). Interannual variability in the subtropical CO_2 flux can also be illustrated by combining data from BATS with those from the nearby Station "S" that exist since 1983 (Keeling, 1993; Gruber et al., 2002; Bates, 2007), with the most recent results finding a peak-to-peak range of ± 0.2 to $0.3\,\mathrm{Pg\,C\,yr^{-1}}$ (Bates, 2007) when scaled to the Northern subtropical gyre. In the eastern subtropical gyre at ESTOC, a weak sink is observed in some years, e.g. 2002, whereas in other years, e.g. 2003, the net sea-air flux is close to zero (Santana-Casiano et al., 2007). Year-to-year variability in the carbon sink at both sites is significantly correlated with sea surface temperature and mixed layer depth anomalies (Gruber et al., 2002; González-Dávila et al., 2007; Santana-Casiano et al., 2007). These were found to be correlated to the NAO without a time lag at BATS (Gruber et al., 2002), and with a 3 yr time lag at ESTOC (Santana-Casiano et al., 2007). With a coupled physical-biogeochemical model, (Oschlies, 2001) illustrated mechanistically that during high (low) NAO phases, the subtropics were subject to less (more) winter mixing bringing up less (more) nutrients to the surface, thereby dampening (strengthening) the seasonal cycle of sea-air fluxes of CO_2 and hence resulting in weaker (stronger) carbon sinks, a prediction confirmed by the observations from BATS (Gruber et al., 2002).

The nearly 30 yr long time series of observations at BATS/Station "S" also indicate that the long-term mean CO_2 sink has remained relatively steady (Bates, 2007). At ESTOC, the rise of surface water pCO_2 between 1996 and 2006 ($1.55 \pm 0.43\,\mu\mathrm{atm\,yr^{-1}}$) was also comparable to the rise in atmospheric CO_2, implying that the long-term mean oceanic sink has also remained relatively constant (González-Dávila et al., 2007).

BGD
9, 10669–10724, 2012

However, the model of Ullman et al. (2009) indicates a steadily increasing sink for CO_2 in the subtropics between 1992 and 2006, in addition to variable climatically-driven changes in convective mixing, biological fluxes and freshwater forcing. Some observational studies have suggested a decreasing CO_2 sink in recent years. A slight weakening of the oceanic sink for carbon was found in the Eastern North Atlantic subtropical waters and the Canaries Current between 2000 and 2008 (Padin et al., 2010). Moreover, Watson et al. (2009) showed that significant interannual variability of the sea-air flux of CO_2 exists throughout the subtropical and temperate zone (30° N–45° N) between 2002 and 2007. Similar to their subpolar biome, McKinley et al. (2011) find decadal climate variability is the best explanation for these observed changes in the subtropics over short temporal extents.

With respect to longer timescale trends, climate-change modeling studies indicate that warming-induced reduction of CO_2 solubility will decrease the ocean carbon uptake, particularly early in the anthropocene (Sarmiento and Le Quéré, 1996) and with pronounced effects in the North Atlantic (Le Quéré et al., 2010). Observations indicate that since 2007 this long-term negative feedback has begun to modify carbon uptake in the North Atlantic subtropical gyre (McKinley et al., 2011).

1.4 The equatorial Atlantic

The equatorial Atlantic is subject to equatorial upwelling (Andrie et al., 1986), seasonal variations (warming/cooling, seasonal migration of the Inter Tropical Convergence Zone), interannual variability probably linked to ENSO events (Philander, 1986), and river discharge (Jacobson et al., 2007). The equatorial Atlantic from 14° N to 15° S is the second most intense source of oceanic CO_2 flux into the atmosphere after the equatorial Pacific, due to frequent upwelling of cold, CO_2-rich water in the Eastern Atlantic which then propagates westward, increasing the fugacity (and therefore flux rate) as it warms (Oudot et al., 1995). Takahashi et al. (2009) estimated the total flux in this region to be $+0.10\,\mathrm{Pg\,C\,yr^{-1}}$ for 2000, although this is likely to be an underestimate because there is a strong north-south gradient of oceanic CO_2 levels, with values in

BGD
9, 10669–10724, 2012

the south up to four times larger than in the north, which is not well reproduced by the climatology (Koffi et al., 2010; Parard et al., 2010). Taking this gradient into account leads to estimates of the flux in this region equating to a source of $+0.22\,\mathrm{Pg\,C\,yr^{-1}}$ (Parard et al., 2010). This outgassing is today only half as large as it used to be in pre-industrial times, since the outgassing of natural CO_2 is substantially counteracted by a strong uptake of anthropogenic CO_2 (Gruber et al., 2009). These authors also suggested that a substantial part of the natural outgassing is the result of the large input of organic matter by rivers, which is then remineralized in this region and subsequently lost to the atmosphere (see also Jacobson et al., 2007). There are few data, and thus estimates of interannual variability or long-term trends have not previously been made; and previous analyses of coupled physical-biogeochemical models have not addressed this region. The RECCAP equatorial Atlantic region has been set to be between 18° S and 18° N, therefore includes the equatorial Atlantic (5° S to 5° N) and the Northern and Southern Tropical Atlantic.

1.5 The Subtropical South Atlantic

The Subtropical South Atlantic is a sink for atmospheric CO_2. Half of this sink appears to be driven by the uptake of anthropogenic CO_2 and the other half by the uptake of natural CO_2 (Gruber et al., 2009). The region is scantily sampled. According to Ito and co-workers (Ito et al., 2005), the isotherm of 23 °C in the South Atlantic Tropical gyre (sSTG) is the boundary between oceanic waters acting as a sink or a source of atmospheric CO_2. Thus, the western sSTG, north of 31° S, acts as a source ($+0.6\,\mathrm{mol\,m^{-2}\,yr^{-1}}$) in boreal spring and as a small sink ($-0.2\,\mathrm{mol\,m^{-2}\,yr^{-1}}$) in autumn, estimated from observations between 2000 and 2008 (Padin et al., 2010). Further south, the region acted as a CO_2 sink of −0.9 and $-2.2\,\mathrm{mol\,m^{-2}\,yr^{-1}}$ in boreal spring and autumn, respectively (Padin et al., 2010). Similar behavior is observed in the Eastern Subtropical South Atlantic (Santana-Casiano and González-Dávila, 2009; González-Dávila et al., 2009): north of 20° S the waters were a source in 2006/2007 ($+0.33\,\mathrm{mol\,m^{-2}\,yr^{-1}}$), and south of 20° S the waters were a sink in

BGD
9, 10669–10724, 2012

2006/2007 ($-0.45\,mol\,m^{-2}\,yr^{-1}$ between 24° S and 20° S, and $-1.89\,mol\,m^{-2}\,yr^{-1}$ between 32° S and 29° S). Estimates of interannual variability or long-term trends are rare. The interannual variability in eastern part of the Southern Subtropical Atlantic has been shown to be large, predominately caused by strong upwelling events (González-Dávila et al., 2009). One study of cruises conducted between 2000 and 2008 in the western part of the Subtropical South Atlantic did not reveal any significant long-term trend of CO_2 uptake in this area (Padin et al., 2010); and previous analyses of coupled physical-biogeochemical models have not addressed this region.

2 Methods

Consistent with the RECCAP methodology, we use global "Tier 1" methodologies for our primary analysis (Canadell et al., 2011). These are sea-air CO_2 fluxes from (1) a sea surface pCO_2 climatology, (2) ocean inversions, (3) atmospheric inversions, and (4) ocean biogeochemical models. Additionally, we use flux estimates based on the gridded product of monthly sea surface observations of fCO_2 from the Surface Ocean CO_2 ATlats (SOCAT) and fluxes estimated at the regional scale based on the pCO_2 database analysis of McKinley et al. (2011). In the Subtropical North Atlantic, we also compare fluxes based on sea surface pCO_2 observations at BATS and at ESTOC.

Throughout, when referring to "fluxes", it refers to contemporary fluxes, i.e. the total flux that is the sum of natural fluxes, fluxes resulting from riverine inputs, and the perturbation due to anthropogenic carbon accumulation in the atmosphere (Gruber et al., 2009).

2.1 Tier 1 RECCAP methodologies

The ocean pCO_2 *climatology* is that produced by Takahashi et al. (2009) for the reference year 2000, based on pCO_2 observations mostly collected between the 1990s and the 2000s. The CO_2 flux was estimated by (Wanninkhof et al., 2012) using Cross

BGD
9, 10669–10724, 2012

Calibrated Multi-Platform wind speeds (CCMP, (Atlas et al., 2011). Uncertainty is estimated conservatively as 50 % of the long-term mean regional flux (Takahashi et al., 2009; Gruber et al., 2009).

Eleven *atmospheric inversions* are included in the analysis (Table 1), retrieved from the TRANSCOM website (https://transcom.lsce.ipsl.fr/). Atmospheric inversions use atmospheric transport models and measured atmospheric CO_2 levels to assess sources and sinks. All fluxes were reported as flux densities in units of ($mol\,m^{-2}\,yr^{-1}$) and we converted fluxes in units of ($Pg\,C\,yr^{-1}$) based on each model's unique land/ocean mask. As the individual atmospheric inversions use the pCO_2 climatology and/or ocean inversions as Bayesian priors, their results are not fully independent from these other methodologies.

Six *ocean biogeochemical models* are included in the analysis, retrieved from the RECCAP website (http://www.globalcarbonproject.org/reccap/products.htm); details are given in Table 2. Ocean biogeochemical models are numerical solutions for ocean circulation and biogeochemical processes that allow for calculation of ocean pCO_2 from total alkalinity (TA) and dissolved inorganic carbon (DIC). Outputs included in this study are monthly CO_2 fluxes of hindcast scenarios forced with historical atmospheric boundary conditions (winds and fluxes of heat and freshwater) and atmospheric pCO_2 concentrations (identified as "ANTH" in the archive). Developers of the CCSM-ETH and UEA simulations submitted alternate model versions to the RECCAP archive, but are not considered here because they were submitted to allow for sensitivity analyses to study the impact of different formulations of the gas-transfer velocity (CCSM-ETHk19) or the impact of different atmospheric forcings (UEA). All fluxes were reported in units of flux density ($mol\,m^{-2}\,yr^{-1}$) and converted to fluxes in units of ($Pg\,C\,yr^{-1}$) based on the each model's unique land/ocean mask.

For a complete closure of the carbon budget with respect to land and globe, carbon fluxes from rivers must be included in ocean model fluxes if those models do not already include them: BER, CSI, BEC, and ETHk15. For these we use the regional, annual mean estimates of (Jacobson et al., 2007), based on the 11 region

BGD
9, 10669–10724, 2012

TRANSCOM mask. In that study, the Arctic and North Subpolar is one region with a total estimate of 0.064 $Pg\,C\,yr^{-1}$ river input, so it must be subdivided for our study (see geographical subregions in Sect. 2.3 below). Following (Rachold et al., 2004), we attribute 0.030 $Pg\,C\,yr^{-1}$ of this to the Arctic and the remainder to the North Subpolar. The net carbon input from rivers into the open ocean is assumed to outgas completely to the atmosphere within the regions of inputs (Jacobson et al., 2007; Gruber et al., 2009).

The *ocean inversion product* of (Gruber et al., 2009) is used. The ocean inversion constrains surface air-sea fluxes based on estimates of the interior ocean circulation and the divergence of surface DIC. Results are taken from the native set of 23 regions of (Gruber et al., 2009), with the long-term mean and average for flux estimates for years 1995, 2000, and 2005 as provided in the RECCAP archive. We use the best-estimate fluxes reported by Gruber et al. (2009) that are a weighted mean result of a set of inversions using 10 different ocean general circulations models that are used to estimate transport of tracers through the ocean. The fluxes for 2000 and 2005 were computed by scaling the anthropogenic CO_2 fluxes reported for 1995 by Gruber et al. (2009) by a factor of 1.109 for the year 2000 and by a factor of 1.23 for 2005, commensurate with the anthropogenic CO_2 flux scaling used in the inversion (Mikaloff Fletcher et al., 2006). The uncertainties are those reported by Gruber et al. (2009). These results were provided for each region in units of ($Pg\,C\,yr^{-1}$), and flux densities in units ($mol\,m^{-2}\,yr^{-1}$) were estimated using the RECCAP area mask (Table 3).

2.2 Observations

From *SOCAT* (Pfeil et al., 2012; Sabine et al., 2012), we use the gridded monthly un-weighted sea surface CO_2 fugacity (fCO_2) product of version 1.5 (http://www.socat.info/), which is on a 1° latitude × 1° longitude grid. Data cover the time period from 1990 to 2007. In order to produce a basin-wide estimate of the flux based on the gridded SOCAT product, a multi-parameter regression (MPR) was performed, using NCEP/NCAR Reanalysis sea surface temperature (Kalnay et al., 1996), SeaWiFS chlorophyll *a*, total

BGD
9, 10669–10724, 2012

alkalinity from the climatology of (Lee et al., 2006), and mixed-layer depth from the climatology of (De Boyer Montegut et al., 2004) as independent parameters. The MPR was performed separately for each of the Atlantic RECCAP regions (see Sect. 2.3 below), including all available years. The root mean square error (RMSE) of the *SOCAT MPR* was 19.9 µatm, computed by comparing the regression-derived values with the original SOCAT product for the Atlantic. No chlorophyll *a* data were available in the Arctic, so that this region is excluded from the SOCAT MPR. Because SeaWiFs chlorophyll *a* was not available the end of 1997 and SOCAT v1.5 ends in 2007, the SOCAT MPR product is produced for years 1998 to 2007. It should be noted that the independent parameters used do not explicitly allow for the increase of surface fCO_2, and the SOCAT MPR is therefore excluded from the trend analysis (Sect. 3.4).

SOCAT MPR flux values were calculated using the standard formulation:

$$F = ks\Delta fCO_2 \quad (1)$$

where k is the gas transfer velocity, s the solubility, and ΔfCO_2 the difference between the atmospheric and oceanic fCO_2. The gas transfer velocity k was calculated using the wind formulation by (Wanninkhof, 1992) with bomb ^{14}C corrections by (Sweeney et al., 2007). Wind speed data, taken from the 6-hourly CCMP Wind Vector Analysis data set (Atlas et al., 2011) were provided for the RECCAP project (Wanninkhof et al., 2012). The solubility s was calculated according to the method presented by (Weiss, 1974), using the in situ temperature and salinity values recorded with each measurement. Atmospheric xCO_2 values were obtained from the reference matrix of GLOBALVIEW (varying over time and latitude, GLOBALVIEW-CO_2, 2011), regridded and converted into fCO_2 using NCEP/NCAR sea level pressure and sea surface temperatures (Kalnay et al., 1996). This resulted in varying atmospheric pCO_2 over time, latitude, and longitude, due to the variability of sea level pressure and sea surface temperature. ΔfCO_2 was then computed as sea surface pCO_2 minus atmospheric pCO_2. Uncertainty is estimated as 50 % of the regional mean flux for the SOCAT fluxes.

BGD
9, 10669–10724, 2012

Additionally, we include an analysis of regional CO_2 fluxes and trends based on the observed in-situ pCO_2 *database* of Takahashi et al. (2009) using the method of (McKinley et al., 2011) adapted to the regions for this analysis (Sect. 2.3). In the North Subpolar region, we also include pCO_2 calculated from direct observations of DIC, TA, SST, and salinity between Iceland and Newfoundland (SURATLANT) of Metzl et al. (2010). In this approach, in situ observations of surface ocean pCO_2 are collapsed onto a single timeseries for each region, and then a harmonic seasonal cycle and a linear trend is fit. The validity of the resulting estimate of the pCO_2 trend is tested through a comparison of pCO_2 trends calculated with the same method using the output from the RECCAP ocean biogeochemical models, sub-sampled at the times and locations of the field observations, compared to pCO_2 trends derived from the complete model fields. Results vary by region, with at least 50 % and up to 100 % of the models confirming that the methodology can capture pCO_2 trends. CO_2 fluxes are estimated with ocean pCO_2 estimated in each month based on the function fit above; atmospheric pCO_2 based on (GLOBALVIEW-CO_2, 2011), integrated over each region; CCMP wind speeds (Wanninkhof et al., 2012) integrated over each region and including the wind speed variance; and Had1SST SST (Rayner et al., 2003). Uncertainty for the fluxes are calculated from the same calculations as above and with trend replaced by the $\pm 1\sigma$ confidence intervals of the trend fit.

At *BATS*, we calculate surface pCO_2 using sea surface measurements of DIC, TA, SST, and salinity, applying CO2SYS (Lewis and Wallace, 1998) with the dissociation constants by (Mehrbach et al., 1973), refitted by (Dickson and Millero, 1987). Data cover the time period from 1990 to 2009. At *ESTOC*, we use sea surface pCO_2 measurements from 1995 to 2009. Fluxes are estimated at BATS and ESTOC in the same way as for SOCAT MPR. For the seasonal cycle, we compare BATS and ESTOC flux densities (mol m^{-2} yr^{-1}) to the other methodologies. For interannual variability, and only for the purpose of comparison, we show BATS and ESTOC fluxes in Pg C yr^{-1} where the area of the entire subtropical region has been used to convert flux densities to

BGD
9, 10669–10724, 2012

fluxes. This is an illustrative comparison to address the issue of how representative these two timeseries are of the entire subtropical basin.

2.3 Geographical subregions

For the purpose of this study, the Arctic and Atlantic are divided geographically into 5 different regions (Table 3, Fig. 1). The North Subtropics, equatorial, and South Subtropics are regions 6, 7 and 8, respectively, of the 11-region TRANSCOM mask (Gurney et al., 2008), whilst the Arctic and North Subpolar are regions 1 and 2, respectively, of the 23-region mask of the Ocean Inversion Project (OIP, Gruber et al., 2009). In Table 3 are the latitudinal and longitudinal boundaries and standard region areas using the RECCAP area mask prepared by N. Gruber on the basis of a global 1° topography and provided in the RECCAP archive (http://www.globalcarbonproject.org/reccap/). There is no one single set of region boundaries used by studies of Atlantic and/or Arctic CO_2 fluxes, hence the boundaries used here are sometimes different to those in other publications.

2.4 Statistics

A quantitative best-estimate flux for the atmospheric inversions and ocean biogeochemical models is derived at by combining all model results in each of these respective methodology, and computing a cross-model median and median absolute deviation (MAD) for the flux ($Pg\,C\,yr^{-1}$) for each month and region. These fluxes were then converted into flux densities ($mol\,m^{-2}\,yr^{-1}$), using the total region area (last column Table 3). Given the variable start and end years for atmospheric inversions, median results are only considered from 1995 to 2008.

When averaging in time for the derived medians of the atmospheric inversions and ocean biogeochemical models and for the other four methodologies that offer only one realization each, a temporal mean is calculated. For the atmospheric inversions, we

BGD
9, 10669–10724, 2012

assume that these mean fluxes are representative of the full period of interest, 1990 to 2009.

Interannual variability for low frequency (multi-annual) variability is calculated by applying a 12-month box filter to each realization of each methodology. High frequency (sub-annual) interannual variability, presented only in Supplement, is calculated for each realization of each methodology by removing a climatological seasonal cycle. For the atmospheric inversions and ocean biogeochemical models, medians are taken after filtering. For consistency with previous studies, uncertainty in the interannual variability is estimated as a standard deviation for each methodology, following the calculation of the median in the case of the atmospheric inversions and ocean models. For trends, we fit a linear trend to the low frequency variability for each methodology, and present the 95 % confidence interval on this fit. In this manuscript, the term *standard error propagation* indicates the square root of the sum of squares in the case of a sum, or the quare root of the mean of the squares in case of a mean. This is a conservative estimate of the uncertainty that does not explicitly exclude the possibility of correlated errors in the estimates.

3 Results

3.1 Long-term mean

Figure 2 shows the long-term temporal mean CO_2 flux density (mol m^{-2} yr^{-1}) at 1° × 1° resolution for the Tier 1 methodologies: the pCO_2 climatology, the weighted mean of the ocean inversions, the median of the atmospheric inversions, and the median of the ocean biogeochemical models; additionally, we show the long-term temporal mean of the gridded SOCAT gridded product and the SOCAT MPR.

All show the strong LTM sink at high latitudes and the net source near the equator. In the main Arctic basin the flux is near zero or set to zero due to (i) ice cover in the models, (ii) the climatology being only equator-wards of 80° N, (iii) limited number of

BGD
9, 10669–10724, 2012

observations in the SOCAT gridded product, and (iv) chlorophyll *a* not being available year-round for the SOCAT MPR.

In Fig. 3 and Table 4, the 1990 to 2009 long-term temporal mean CO_2 flux ($Pg\,C\,yr^{-1}$) is presented by region and by methodology. For each region, the methodologies agree as to the sign of the flux, and generally also as to the magnitude when the uncertainty is considered. The Arctic has a neutral flux or a small sink of up to $-0.05 \pm 0.03\,Pg\,C\,yr^{-1}$. The North Subpolar region has the widest range of estimates, ranging from -0.07 to $-0.30\,Pg\,C\,yr^{-1}$. The sink in the North Subtropics ranged from $-0.13\,Pg\,C\,yr^{-1}$ to $-0.34\,Pg\,C\,yr^{-1}$. The equatorial region is a source, with fluxes ranging from $0.10\,Pg\,C\,yr^{-1}$ to $0.15\,Pg\,C\,yr^{-1}$. The South Subtropics is a sink of atmospheric CO_2, ranging from $-0.10\,Pg\,C\,yr^{-1}$ to $-0.25\,Pg\,C\,yr^{-1}$. For the whole Atlantic and Arctic region, the sink estimates ranged from $-0.37\,Pg\,C\,yr^{-1}$ to $-0.64\,Pg\,C\,yr^{-1}$.

The best estimate of the flux (Table 4) for the four Atlantic regions are an average of the pCO_2 climatology and of the ocean inversion, selected because they are two independent data-based estimates: for the North Subpolar $-0.21 \pm 0.06\,Pg\,C\,yr^{-1}$, for the North Subtropics $-0.26 \pm 0.06\,Pg\,C\,yr^{-1}$, for the Equatorial $0.12 \pm 0.04\,Pg\,C\,yr^{-1}$, and for the South Subtropics $-0.14 \pm 0.04\,Pg\,C\,yr^{-1}$. In the Arctic, the Tier 1 methodologies do not offer reliable flux estimates because they are based on limited data that may not be representative of the entire region (pCO_2 climatology, ocean inversion, and atmospheric inversions) and/or are poorly resolved in the underlying physical and/or biogeochemical models (ocean inversion, atmospheric inversion and ocean biogeochemical models). Therefore, we do not use these estimates as part of the long-term mean best estimate. Instead, we take the range of reported Arctic Ocean CO_2 uptake from the literature, as discussed in Sect. 1.1: $-0.12 \pm 0.06\,Pg\,C\,yr^{-1}$.

3.2 Seasonal cycle

The zonal Atlantic mean seasonal cycles of the CO_2 flux densities ($mol\,m^{-2}\,yr^{-1}$) are presented in Fig. 4 for the Tier 1 methodologies: pCO_2 climatology, atmospheric

BGD
9, 10669–10724, 2012

inversion median, and the ocean biogeochemical model median; additionally we show the result for the observations-based SOCAT MPR. The ocean inversions only give annual mean fluxes, and thus are not shown. The fluxes in the South Subtropics, equatorial region, and North Subtropics follow the mainly temperature driven increase in pCO_2 in the warmer summer months, which results in outgassing in summer. Polewards of 44° N, the SOCAT MPR (Fig. 4d) shows an outgassing in winter, similar to an observational study for 2005 (Watson et al., 2009; Olsen et al., 2008; Chierici et al., 2009). This is also evident to a minor degree by the pCO_2 climatology (Fig. 4a), yet is not found in the other Tier 1 methodologies.

The spatial mean seasonal cycles of the CO_2 flux densities (mol m^{-2} yr^{-1}) for each region are shown in Fig. 5 for Tier 1 methodologies: pCO_2 climatology, atmospheric inversions' median, and ocean biogeochemical models' median; additionally, we include results from the SOCAT MPR and pCO_2 database methods (all regions except the Arctic). We include BATS and ESTOC in the North Subtropics.

In Table 5, we present the correlation coefficients for the seasonal cycles in each region.

In the *Arctic* (Fig. 5a), all three methods have near zero fluxes for most of the year due to ice-cover, and a small drawdown in summer, which leads to good correlation of the pCO_2 climatology to the atmospheric inversions and ocean biogeochemical models (Table 5a). The ocean biogeochemical models and atmospheric inversion cycles do not correlate well.

In the *North Subpolar* region (Fig. 5b), the seasonal cycle is the most intense of all the regions. There is agreement in the shape and amplitude of the seasonal cycle of the ocean biogeochemical models and the pCO_2 climatology, with a seasonal cycle influenced by a mixed temperature-driven and biologically-driven pCO_2 cycle in this region (Takahashi et al., 2002; Bennington et al., 2009). However, the seasonal cycle of the ocean biogeochemical models is more dominated by the temperature component in summer compared to that of the pCO_2 climatology. The SOCAT MPR shows the opposite seasonal cycle (Fig. 5b), with an efflux in winter and a sink in summer,

BGD
9, 10669–10724, 2012

indicating a biologically-dominated mean seasonal cycle. This pattern is consistent with detailed studies in the subpolar gyre (Chierici et al., 2009; Olsen et al., 2008; Watson et al., 2009; Rödenbeck et al., 2012). However, the mean SOCAT MPR sink is much lower than that of the other methodologies (Fig. 3b). It should be noted, however, that the SOCAT MPR only extends to 65° N, hence does not cover the whole of the RECCAP subpolar region. This predominantly biologically driven season cycle is also evident in the pCO_2 database approach, which is notable because, even though a significant amount of data is common between SOCAT and Takahashi et al. (2009), the data treatment to derive the RECCAP regions' surface pCO_2 values are quite different (Sect. 2.2). Finally, the atmospheric inversions have a seasonal cycle that is significantly out of phase with the ocean models, with their median peaking in September, most possibly due to the significant terrestrial influence in this region bordered by large continents. The spread of their seasonal cycle is very large, with a lack of consistency in the shape of the cycle across the set (not shown).

With a boundary defined simply by the latitude of 49° N, the RECCAP North Subpolar region is not well-defined based on the actual physical and biogeochemical state of this region (McKinley et al., 2011; Sarmiento et al., 2004). The choice of this boundary is historical, out of the TRANSCOM effort, and we use it for consistency with the overall RECCAP process. Yet, this choice means that the seasonal cycle from the methodologies with full spatial coverage (ocean models, pCO_2 climatology) are not dominated by biological activity, i.e. winter convective mixing brings DIC into surface waters and biological productivity removes it in summer, as it should be. That fluxes are closer to zero in summer suggests a strong temperature control, likely due to the inclusion of the northern reaches of the subtropical gyre (Fig. 4).

In the *North Subtropics* (Fig. 5c), all methodologies are well correlated, with the correlation coefficient, R, ranging from 0.94 to 1, such that we can consider this cycle to be well-known. Nevertheless, we note that amongst the Tier 1 methodologies, the ocean biogeochemical models have a larger efflux in late summer and fall than in the pCO_2 climatology and the atmospheric inversions. Because of regular monthly sampling, fluxes

BGD
9, 10669–10724, 2012

at BATS and ESTOC are known with high confidence, with the eastern subtropical region (ESTOC) showing a shallower mean seasonal cycle than the western subtropical regions (BATS).

Observations in the RECCAP *equatorial* Atlantic, south of the equator at the PIRATA mooring at 6° S/10° W, show that the CO_2 flux ranges from 0.4 mol m^{-2} yr^{-1} in June to a maximum of 2.4 mol m^{-2} yr^{-1} in March and October. However, the amplitude of the temporal mean seasonal cycle of the CO_2 flux in the whole equatorial Atlantic is small (Fig. 5d) because the seasonal cycles of Northern and Southern Hemispheres cancel each other out. Correlation coefficients between methodologies are low, in part because of the lack of a substantial seasonal signal. Still, we note that all these methodologies have difficulties in this region. Limited tropical atmospheric CO_2 data makes capturing the seasonal cycle a challenge for atmospheric inversions. Tropical ocean dynamics are poorly represented in ocean biogeochemical models, and there is limited data for model calibration and validation here. There are limited in situ pCO_2 observations from which the pCO_2 climatology (Takahashi et al., 2009), SOCAT MPR and pCO_2 database estimates are derived.

The seasonal cycles of the *South Subtropics* (Fig. 5e) agree well across methodologies, with correlations all being statistically significant. We note the similar patterns of the mean seasonal cycles shown by the atmospheric inversions and the pCO_2 climatology, which should be largely due to the atmospheric inversions using these same climatological CO_2 fluxes as a prior and there being very limited atmospheric pCO_2 data in the temperate Southern Hemisphere to move results away from the priors.

3.3 Inter-annual variability (IAV)

Figure 6 shows the low-frequency IAV and trends for Tier 1 methodologies for the atmospheric inversions, ocean biogeochemical models, and the pCO_2 database. High-frequency IAV can be found in the Supplement. Note that fluxes at BATS and ESTOC in (Pg C yr^{-1}) are assuming the same flux intensities of each site at each grid point in the whole RECCAP subtropical region.

BGD
9, 10669–10724, 2012

In Table 6, the amplitude of the interannual variability (IAV) is presented for each approach, calculated as the temporal standard deviation. SOCAT MPR IAV is compared here even though it is not shown in Fig. 6. Variability is smallest in the Arctic (0.0030 to 0.0046 $\mathrm{Pg\,C\,yr^{-1}}$) and largest in the North and South Subtropics (up to 0.026 $\mathrm{Pg\,C\,yr^{-1}}$). The atmospheric inversions suggest the largest variability, and the SOCAT MPR the smallest. The integrated Arctic/Atlantic regional sink varies by $\pm 0.055\,\mathrm{Pg\,C\,yr^{-1}}$ for the atmospheric inversions, $\pm 0.029\,\mathrm{Pg\,C\,yr^{-1}}$ in the ocean biogeochemical models, $\pm 0.015\,\mathrm{Pg\,C\,yr^{-1}}$ in the SOCAT MPR, and $\pm 0.046\,\mathrm{Pg\,C\,yr^{-1}}$ in the pCO_2 database.

Correlation of the low frequency interannual variability is presented in Table 7 by region. On the whole, correlations are low. In some regions and between some methods, there are significant and positive correlations, but there is not a consistent pattern of strong positive correlations between methods across all regions. For the whole Atlantic and Arctic, the highest positive correlation (0.87) is between the SOCAT MPR and the pCO_2 database, and this is due to high positive correlations in the North Subpolar and South Subtropics regions. As for the seasonal cycle, this is encouraging because though these estimates are derived from very similar datasets of in situ pCO_2 the methodologies used to interpolate through space and time are quite different.

It is notable that the NAO has highest correlations to the Tier 1 results in the equatorial and South Subtropics regions, but generally weak and insignificant correlations across the North Atlantic.

In the North Subtropics, BATS positively correlates to all the other methodologies, which suggests that this location is somewhat representative of carbon fluxes across the gyre. Lower and insignificant correlations at ESTOC indicate that it is less representative of the large-scale behaviour.

Atmospheric inversions may mistakenly attribute interannual variability of terrestrial fluxes to oceanic flux variability, because the atmospheric signals are dominated by the larger terrestrial variability. However, when individual realizations of the atmospheric inversions and ocean biogeochemical models are correlated (not shown), some strong and statistically significant correlations ($p < 0.05$) are found in all regions. Thus, even

BGD
9, 10669–10724, 2012

though the medians across the methodologies do not necessarily correlate strongly (Table 7), some of the individual realizations of atmospheric inversions and ocean biogeochemical models do share signals of multi-year variability.

3.4 Linear trends of the sea-air CO_2 flux

Table 8 presents the linear trends of the sea-air CO_2 flux for 1995–2009 in each region from the atmospheric inversions, ocean biogeochemical models, and observations-based trends from the pCO_2 database. The SOCAT MPR is not included as its time-period is shorter than this.

For 1995 to 2009, linear trends are generally negative, indicating an increasing sink, or indistinguishable from zero. The exception is the equatorial Atlantic and South Subtropics where positive trends for the atmospheric inversion indicate increasing outgassing, while for the same regions the ocean biogeochemical models trends are neutral and the pCO_2 database trends are negative. For the whole Atlantic and Arctic, the atmospheric inversions suggest a steady sink while the ocean models and pCO_2 database suggest an increasing sink, with the basin scale difference driven by the equatorial region. The strong increasing trend for the pCO_2 database is dominated by the trend in the South Subtropics where data are extremely limited. Even in other regions, the pCO_2 database method suggests the largest trends, and should be considered upper-bound estimates for the trends because this approach estimates the fluxes from a repeating harmonic seasonal cycle and a steadily changing, linear trend in pCO_2 over the full time period, i.e. interannual variability in pCO_2 is suppressed (Sect. 2.2).

4 Discussion

Taking the sum of the best estimates for each region (selected as the pCO_2 climatology and the ocean inversion), the 1990 to 2009 long-term mean sea-air flux for the Arctic +

BGD
9, 10669–10724, 2012

Atlantic is estimated to be $-0.61 \pm 0.13\,\mathrm{Pg\,C\,yr^{-1}}$, which makes the region responsible for 36 % of the global contemporary uptake of $-1.7 \pm 0.10\,\mathrm{Pg\,C\,yr^{-1}}$ as estimated by ocean inversion (Gruber et al., 2009).

4.1 The Arctic

Our assessment of the long-term mean flux in the Arctic is derived from previous literature due to the poor representation of the Arctic in the Tier 1 RECCAP methodologies and basin-scale data products that are the focus of this paper. This estimate is a net sea-air flux of $-0.12 \pm 0.06\,\mathrm{Pg\,C\,yr^{-1}}$. With respect to the seasonal cycle, there is some agreement in the Tier 1 methodologies as to the shape of this cycle, indicating the largest seasonal drawdown in summer when sea ice is at a minimum, a result that is mechanistically sensible. Given concerns about the Tier 1 methodologies in their ability to represent the long-term mean flux in the Arctic, we cannot put much weight on their assessment of the amplitude of the seasonal cycle, interannual variability, or the long-term trends in CO_2 flux. Multi-annual timescales are also not captured by direct observations, and thus much more work is needed to fully elucidate sea-air CO_2 fluxes and their variability in the Arctic.

Estimates of primary production based on satellite data suggest that decreases in sea-ice extent could have increased the productivity of Arctic waters in the recent years (Arrigo and van Djiken, 2011; Pabi et al., 2008). This could have enhanced the strength of the biological pump of the Arctic Ocean, and driven an increased CO_2 sink (McGuire et al., 2010), an effect also shown in model simulations (Zhang et al., 2010). But this effect may be muted by counteracting impacts on upper ocean carbon chemistry of warming and freshening. With data, Cai et al. (2010) showed that part of the Western Arctic has decreased its CO_2 uptake capacity due to the change in ocean carbon chemistry despite a decrease in sea-ice area. Additionally, ocean acidification may trigger unexpected changes in the biological pump and in CO_2 uptake (Bates and Mathis, 2009). The simultaneous occurrence of multiple and contrasting processes (both physical and

BGD
9, 10669–10724, 2012

biogeochemical) in the Arctic significantly complicates our understanding and prediction of the direction and magnitude of the trend of its CO_2 sink.

4.2 The North Subpolar

The North Subpolar region is a substantial sink for atmospheric CO_2 of $-0.21 \pm 0.06\,Pg\,C\,yr^{-1}$ over the RECCAP period, 1990–2009, despite its small area. Analysis of the ocean inversion (Gruber et al., 2009) suggests that about half of the total long-term mean flux is driven by the uptake of anthropogenic CO_2, and the remainder is due to the natural carbon cycle. The latter is a consequence of reinforcing tendencies from net ocean cooling, which increases the uptake of atmospheric CO_2 by increasing the ocean's solubility, and from a relatively efficient biological pump. This uptake tendency is slightly reduced by the outgassing of carbon supplied by rivers to the ocean.

Mechanistic understanding of the seasonal cycle in the North Atlantic subpolar gyre is as follows: strong biological drawdown in spring, and continued drawdown through summer that opposes the temperature-driven cycle, followed by efflux of respired CO_2 with winter mixing (Takahashi et al., 2009; Watson et al., 2009; Olsen et al., 2008). Estimates of the seasonal cycle of the CO_2 flux in the North Subpolar region agree between the pCO_2 database and the ocean biogeochemical models, but include a significant CO_2 efflux in the summer that is a subtropical, temperature-driven, signal. The RECCAP North Subpolar region, derived from the TRANSCOM project, includes a significant portion of the subtropical gyre, and thus these estimates are affected by the imposed regional boundaries. The atmospheric inversions have a very broad set of estimates for the seasonal cycle, leading to a median with maximum drawdown in September, which is long after the subpolar spring bloom. The two methods based on in situ pCO_2 data have maximum CO_2 uptake at the time of the bloom, and then a relatively flat cycle through the rest of the year. We recommend that future assessments use regional boundaries that are defined by biogeochemical provinces (Sarmiento et al., 2004; McKinley et al., 2011) as opposed to lines of latitude.

BGD
9, 10669–10724, 2012

Interannual variability in the North Subpolar region is small, ranging from 0.004 to 0.016 $Pg\,C\,yr^{-1}$ (Table 6). There is limited correlation between the methodologies, which we partially attribute to regional boundaries being sub-optimal. Maximum correlations come between the pCO_2 database and the other methodologies, which is due largely to the fact that wind speed variability is the only source of interannual variability in the pCO_2 database approach. There are no strong correlations of the variability with the NAO. Trends in CO_2 uptake for 1995–2009 are neutral or negative, indicating a steady or increasing sink. These trends are best interpreted as a response to decadal timescale climate variability given their short timeframes (McKinley et al., 2011).

4.3 The North Subtropics

The North Subtropics is a significant long-term sink for atmospheric CO_2 at $-0.26 \pm 0.06\,Pg\,C\,yr^{-1}$ between 1990 and 2009, driven by a substantial uptake flux of anthropogenic CO_2 and a natural CO_2 uptake driven in turn by net heat loss and the biological pump. This sink ($-0.93\,mol\,C\,m^{-2}\,yr^{-1}$, Table 4) is substantiated by the observation-based flux estimates in the Western Subtropical Atlantic at BATS between 1983 and 2005 ($-0.8 \pm 0.2\,mol\,m^{-2}\,yr^{-1}$ and $-1.2 \pm 0.3\,mol\,m^{-2}\,yr^{-1}$, Bates, 2007); the sink in the Eastern Subtropical Atlantic at ESTOC was lower between 1995 and 2004 at $-0.05 \pm 0.03\,mol\,m^{-2}\,yr^{-1}$ (Santana-Casiano et al., 2007). The seasonal cycle in the subtropics is mainly temperature driven, with an efflux in summer and an uptake in winter, being influenced to a small degree by low biological activity. All methodologies show the same patterns, which are significantly correlated (Table 5c). The ocean biogeochemical models show maximum summer efflux being notably larger and later compared to that of other methodologies. This class of ocean biogeochemical models tends to underestimate biological productivity in the stratified subtropical gyre. This leads to excessive late summer and fall surface ocean pCO_2 and too large an efflux at this time of year, and this also biases the long-term mean uptake of the ocean biogeochemical models to be too low (Table 4, Fig. 3). The Eastern subtropical region

BGD
9, 10669–10724, 2012

shows a smaller mean seasonal cycle compared to the western region (ESTOC and BATS, respectively (Fig. 5), as has previously been shown (Bates, 2007; González-Dávila et al., 2007). Consistent with findings of the interannual variability, the seasonal cycle at BATS is more representative of the majority of this basin region compared to the seasonal cycle at ESTOC.

Interannual variability in the North Subtropics ranged from 0.008 to 0.026 $Pg\,C\,yr^{-1}$ (Table 6), with the atmospheric inversions showing the largest and the SOCAT MPR showing the lowest value. Our estimate of peak-to-peak IAV in the subtropical gyre based only on observations at BATS (Fig. 6e) is consistent with a previous estimate for 1983–2005 of 0.2–0.3 $Pg\,C\,yr^{-1}$ (Bates, 2007). At the BATS site, the subtropical mode water (STMW) uptake was approximately $-0.05\,Pg\,C\,yr^{-1}$ in the 1990s, weakening to approximately $-0.02\,Pg\,C\,yr^{-1}$ in the 2000s, most likely related to a shift in the NAO index from positive to neutral/mildly negative in the 2000s (Bates et al., 2012; Levine et al., 2011). The correlation of the interannual variability at BATS with Tier 1 methodologies is statistically significant whilst that at ESTOC is not (Table 7c); as these are instantaneous correlations, these results agree with in-depth studies of the CO_2 fluxes at the two sites (Gruber et al., 2002; Santana-Casiano et al., 2007).

Statistically significant negative linear trends are found for the sea-air CO_2 flux from 1995 to 2009 (Table 8) as determined by the atmospheric inversions, ocean biogeochemical models, and the pCO_2 database, indicating a long-term increase in the CO_2 sink. This is in contrast to results from BATS/Station "S", where the long-term mean fluxes have remained constant over the last 3 decades (Bates et al., 2012). At ESTOC, the rate of increase of surface pCO_2 was higher between 1995 and 2009 (González-Dávila and Santana Casiano, 2012) than between 1995 and 2004 (Santana-Casiano et al., 2007), potentially indicating a decrease in the sink. The time period over which a trend is determined is crucial when comparing different estimates (McKinley et al., 2011).

BGD
9, 10669–10724, 2012

4.4 The equatorial region

The equatorial region is the only net outgassing region in the Atlantic, with a significant long-term source of atmospheric CO_2 of $0.12 \pm 0.04\,Pg\,C\,yr^{-1}$ between 1990 and 2009, with estimates by the different methodologies being indistinguishable from each other. This efflux in the equatorial Atlantic is approximately 6 times smaller than the outgassing in the Tropical Pacific (Gruber et al., 2009). The Atlantic efflux of our study is, however, significantly lower than the ones estimated between 5° S and 5° N between 1982 to 1984 (Andrie et al., 1986), between 10° W–10° E, 10° S–6° N between 2005 and 2007 (Koffi et al., 2010), and at 6° S, 10° W in 2007 (Parard et al., 2010). The RECCAP equatorial Atlantic region includes the equatorial Atlantic (5° S to 5° N), the Northern Tropical Atlantic and the Southern Tropical Atlantic; this leads to an overall small efflux in the whole RECCAP region (18° S to 18° N) by cancelling the source south of the equator and the sink north of the equator (González-Dávila and Santana Casiano, 2012). Additionally, the region suffers from a scarcity of observations, both oceanic and atmospheric, so that significant upwelling events (Andrie et al., 1986) cannot be captured by the observations, and might be under-represented in the models, contributing to the small efflux.

A seasonal cycle in the RECCAP Equatorial is not discernible, as it includes opposing cycles from the Northern and Southern Hemisphere, and the correlations between most methodologies are not statistically significant (Table 5d). Interannual variability in the Tropical Atlantic is probably linked to ENSO events with warm events in the Tropical Atlantic following the occurrence of El Niño events in the Pacific (e.g. Philander, 1986), leading to higher than usual pCO_2 in the equatorial Atlantic associated with higher SST in boreal winter (Andrie et al., 1986). However, it is not clear whether the CO_2 flux would be significantly different, as the increase of surface pCO_2 caused by warming might be counterbalanced by weaker trade winds. The CO_2 flux trend estimates (Table 8) varied in sign and statistical significance; due to the lack of sufficient atmospheric

BGD
9, 10669–10724, 2012

and oceanic observations, we put highest confidence into the estimate by the ocean biogeochemical models, i.e a steady source for 1995 and 2009.

4.5 The South Subtropics

The RECCAP South Subtropics, 44° S to 18° S, is a significant long-term sink for atmospheric CO_2 at $-0.14 \pm 0.04\,Pg\,C\,yr^{-1}$ between 1990 and 2009. It includes areas of net outgassing and net uptake of atmospheric CO_2, bounded along the 23°C isotherm (Ito et al., 2005), visible between 30° S and 20° S in both the long-term mean flux (Fig. 2) and the mean seasonal cycles (Fig. 4). Observations in both the Western South Subtropics (Padin et al., 2010) as well as the Eastern South Subtropics (Santana-Casiano and González-Dávila, 2009; González-Dávila et al., 2009) show this pattern. The South Subtropical seasonal cycle is again mainly temperature driven, with an efflux in summer and an uptake in winter; all methodologies show this pattern, being highly correlated (Table 5e), we therefore know the South Subtropical seasonal cycle with high confidence in this RECCAP region. Interannual variability in this region is large (Fig. 6e), possibly caused by strong upwelling events in the eastern part (González-Dávila et al., 2009). CO_2 flux trend estimates (Table 8) again vary in sign and significance. As this region also suffers from a scarcity of observations, both oceanic and atmospheric, we put highest confidence into the trend estimate by the ocean biogeochemical models which indicates a steady sink over 1995 and 2009.

5 Conclusions

- The long-term net sea-air CO_2 flux in the Atlantic and Arctic was $-0.61 \pm 0.12\,Pg\,C\,yr^{-1}$ between 1990 and 2009.
- The interannual variability of the Atlantic and Arctic basins together ranged from 0.02 to $0.06\,Pg\,C\,yr^{-1}$ between 1990 and 2009.

BGD
9, 10669–10724, 2012

– Trends of the sea-air CO_2 flux varied between time periods and methodologies used. Given highest confidence in the ocean biogeochemical models due to their mechanistic nature, the whole Atlantic and Arctic region had an increasing sink between 1995 and 2009 of $-0.03 \pm 0.01\,\mathrm{Pg\,C\,yr^{-1}}$ decade^{-1}.

– We find broad agreement amongst methodologies in the mean seasonal cycle in the Subtropical Atlantic of both hemispheres, yet not elsewhere.

Supplementary material related to this article is available online at: http://www.biogeosciences-discuss.net/9/10669/2012/bgd-9-10669-2012-supplement.zip.

Acknowledgements. U. Schuster and G. A. McKinley contributed equally to this manuscript and should be considered as joint first-authors. We thank P. Canadell, P. Ciais, C. Le Quéré, and C. Sabine for co-ordinating the global effort of RECCAP. We thank Captains, Officers, and Crew of all ships on which measurements have been made that contribute to this study. U. Schuster has been supported by EU grants IP 511176-2 (CARBOOCEAN), 212196 (COCOS), and 264879 (CARBOCHANGE), and UK NERC grant NE/H017046/1 (UKOARP). G. A. McKinley and A. Fay thank NASA for support (NNX08AR68G, NNX11AF53G). P. Landschützer has been supported by EU grant 238366 (GREENCYCLESII). N. Metzl acknowledges the French national funding program LEFE/INSU. Support for N. Gruber has been provided by EU grants 264879 (CARBOCHANGE) AND 283080 (GEO-CARBON) S. Doney acknowledges support from the NOAA (NOAA-NA07OAR4310098).

References

Anderson, L. G., Dyrssen, D., and Jones, E. P.: An assessment of the transport of atmospheric CO_2 into the Arctic Ocean, J. Geophys. Res., 95, 1703–1711, 1990.

Anderson, L. G., Olsson, K., and Skoog, A.: Distribution of dissolved inorganic and organic carbon in the Eurasian Basin of the Arctic Ocean, in: The Polar Oceans and their Role

BGD
9, 10669–10724, 2012

in Shaping the Global Environment, edited by: Johannessen, O. M., Muench, R. D., and Overland, J. E., Geophysical Monographs, American Geophysical Union, 252–262, 1994.
Anderson, L. G., Jutterstrom, S., Hjalmarsson, S., Wahlstrom, I., and Semiletov, I. P.: Outgassing of CO_2 from Siberian Shelf seas by terrestrial organic matter decomposition, Geophys. Res. Lett., 36, L20601, doi:10.1029/2009GL040046, 2009.
Andrie, C., Oudot, C., Genthon, C., and Merlivat, L.: CO_2 fluxes in the Tropical Atlantic during Focal cruises, J. Geophys. Res., 91, 1741–1755, 1986.
Arrigo, K. R. and van Djiken, G. L.: Secular trends in Arctic Ocean net primary production, J. Geophys. Res., 116, C09011, doi:10.1029/2011JC007151, 2011.
Arrigo, K. R., van Dijken, G., and Pabi, S.: Impact of a shrinking Arctic ice cover on marine primary production, Geophys. Res. Lett., 35, L19603, doi:10.1029/2008GL035028, 2008.
Arrigo, K. R., Pabi, S., van Dijken, G. L., and Maslowski, W.: Air-sea flux of CO_2 in the Arctic Ocean, 1998–2003, J. Geophys. Res., 115, G04024, doi:10.1029/2009JG001224, 2010.
Arrigo, K. R., Perovich, D. K., Pickart, R. S., Brown, Z. W., van Dijken, G. L., Lowry, K. E., Mills, M. M., Palmer, M. A., Balch, W. M., Bahr, F., Bates, N. R., Benitez-Nelson, C., Bowler, B., Brownlee, E., Ehn, J. K., Frey, K. E., Garley, R., Laney, S. R., Lubelczyk, L., Mathis, J., Matsuoka, A., Mitchell, G. B., Moore, G. W. K., Ortega-Retuerta, E., Pal, S., Polashenski, C. M., Reynolds, R. A., Schieber, B., Sosik, H. M., Stephens, M., P., and Swift, J. H.: Massive phytoplankton blooms under Arctic sea icea, Science, 336, 1408, doi:10.1126/science.1215065, 2012.
Assmann, K. M., Bentsen, M., Segschneider, J., and Heinze, C.: An isopycnic ocean carbon cycle model, Geosci. Model Dev., 3, 143–167, doi:10.5194/gmd-3-143-2010, 2010.
Atlas, R., Hoffman, R. N., Ardizzone, J., Leidner, S. M., Jusem, J. C., Smith, D. K., and Gombos, D.: A cross-calibrated multiplatform ocean surface wind velocity product for meteorological and oceanographic applications, B. Am. Meteorol. Soc., 92, 157–174, doi:10.1175/2010BAMS2946.1, 2011.
Aumont, O. and Bopp, L.: Globalizing results from ocean in situ iron fertilization studies, Global Biogeochem. Cy., 20, GB2017, doi:10.1029/2005GB002591, 2006.
Bates, N. R.: Air-sea CO_2 fluxes and the continental shelf pump of carbon in the Chukchi Sea adjacent to the Arctic Ocean, J. Geophys. Res., 111, C10013, doi:10.1029/2005JC003083, 2006.

BGD
9, 10669–10724, 2012

Bates, N. R.: Interannual variability of the oceanic CO_2 sink in the subtropical gyre of the North Atlantic Ocean over the last 2 decades, J. Geophys. Res., 112, C09013, doi:10.1029/2006JC003759, 2007.

Bates, N. R. and Mathis, J. T.: The Arctic Ocean marine carbon cycle: evaluation of air-sea CO_2 exchanges, ocean acidification impacts and potential feedbacks, Biogeosciences, 6, 2433–2459, doi:10.5194/bg-6-2433-2009, 2009.

Bates, N. R., Best, M. H. P., Neely, K., Garley, R., Dickson, A. G., and Johnson, R. J.: Detecting anthropogenic carbon dioxide uptake and ocean acidification in the North Atlantic Ocean, Biogeosciences, 9, 2509–2522, doi:10.5194/bg-9-2509-2012, 2012.

Bennington, V., McKinley, G. A., Dutkiewicz, S., and Ullman, D.: What does chlorophyll variability tell us about export and air-sea CO_2 flux variability in the North Atlantic?, Global Biogeochem. Cy., 23, GB3002, doi:10.1029/2008GB003241, 2009.

Cai, W. J., Chen, L. Q., Chen, B. S., Gao, Z. Y., Lee, S. H., Chen, J. F., Pierrot, D., Sullivan, K., Wang, Y. C., Hu, X. P., Huang, W. J., Zhang, Y. H., Xu, S. Q., Murata, A., Grebmeier, J. M., Jones, E. P., and Zhang, H. S.: Decrease in the CO_2 uptake capacity in an ice-free Arctic Ocean basin, Science, 329, 556–559, 2010.

Canadell, J. G., Ciais, P., Gurney, K., Le Quéré, C., Piao, S., Raupack, M. R., and Sabine, C. L.: An international effort to quantify regional carbon fluxes, EOS, 92, 81–88, 2011.

Chierici, M., Olsen, A., Johannessen, T., Triñanes, J., and Wanninkhof, R.: Algorithms to estimate the carbon dioxide uptake in the Northern North Atlantic using shipboard observations, satellite and ocean analysis data, Deep-Sea Res. Pt. II, 56, 630–639, 2009.

Corbière, A., Metzl, N., Reverdin, G., Brunet, C., and Takahashi, T.: Interannual and decadal variability of the oceanic carbon sink in the North Atlantic subpolar gyre, Tellus B, B, 168–178, 2007.

De Boyer Montegut, C., Madec, G., Fisher, A. S., Lazar, A., and Iudicone, D.: Mixed layer depth over the global ocean: An examination of profile data and a profile-based climatoloy, J. Geophys. Res., 109, C12003, doi:10.1029/2004JC002378, 2004.

Dickson, A. G. and Millero, F. J.: A comparison of the equilibrium constant for the dissolution of carbonic acid in seawater media, Deep-Sea Res., 34, 1733–1743, 1987.

Feely, R. A., Takahashi, T., Wanninkhof, R., McPhaden, M. J., Cosca, C. E., Sutherland, S. C., and Carr, M. E.: Decadal variability of the air-sea CO_2 fluxes in the equatorial Pacific Ocean, J. Geophys. Res., 111, C08S90, doi:10.1029/2005JC003129, 2006.

BGD
9, 10669–10724, 2012

GLOBALVIEW-CO_2: Cooperative Atmospheric Data Integration Project – Carbon Dioxide, CD-ROM, NOAA ESRL, Boulder, Colorado (also available on Internet via anonymous FTP to: ftp://ftp.cmdl.noaa.gov, Path: ccg/co2/GLOBALVIEW), 2011.In this manuscript, the term

González-Dávila, M. and Santana Casiano, J. M.: CO_2 fluxes in the Eastern equatorial Atlantic, in preparation, 2012.

González-Dávila, M., Santana-Casiano, J. M., and Gonzalez-Davila, E. F.: Interannual variability of the upper ocean carbon cycle in the Northeast Atlantic Ocean, Geophys. Res. Lett., 34, L07608, doi:10.1029/2006GL028145, 2007.

González-Dávila, M., Santana Casiano, J. M., and Ucha, I. R.: Seasonal variability of fCO_2 in the Angola-Benguela region, Prog. Oceanogr., 83, 124–133, 2009.

Graven, H. D., Gruber, N., Key, R., Khatiwala, S., and Giraud, X.: Changing controls on oceanic radiocarbon: new insights on shallow-to-deep ocean exchange and anthropogenic CO_2 uptake, J. Geophys. Res., in revision, 2012.

Gruber, N., Keeling, C. D., and Bates, N. R.: Interannual variability in the North Atlantic ocean carbon sink, Science, 298, 2374–2378, 2002.

Gruber, N., Gloor, M., Mikaloff Fletcher, S. E., Doney, S. C., Dutkiewicz, S., Follows, M., Gerber, M., Jacobson, A. R., Joos, F., Lindsay, K., Menemenlis, D., Mouchet, A., Mueller, S. A., Sarmiento, J. L., and Takahashi, T.: Oceanic sources, sinks, and transport of atmospheric CO_2, Global Biogeochem. Cy., 23, GB1005, doi:10.1029/2008GB003349, 2009.

Gurney, K. R., Baker, D., Rayner, P., and Denning, A. S.: Interannual variations in continental-scale net carbon exchange and sensitivity to observing networks estimated from atmospheric CO_2 inversions for the period 1980 to 2005, Global Biogeochem. Cy., 22, GB3025, doi:10.1029/2007GB003082, 2008.

Hakkinen, S. and Rhines, P. B.: Shifting surface currents in the Northern North Atlantic Ocean, J. Geophys. Res., 114, C04005, doi:10.1029/2008JC004883, 2009.

Ishii, M., Inoue, H. Y., Midorikawa, T., Saito, S., Tokieda, T., Sasano, D., Nakadate, A., Nemoto, K., Metzl, N., Wong, C. S., and Feely, R. A.: Spatial variability and decadal trend of the oceanic CO_2 in the Western equatorial Pacific warm/fresh water, Deep-Sea Res. Pt. II, 56, 591–606, 2009.

Ito, R. G., Schneider, B., and Thomas, H.: Distribution of surface fCO_2 and air-sea fluxes in the Southwestern Subtropical Atlantic and adjacent continental shelf, J. Mar. Syst., 56, 227–242, 2005.

BGD
9, 10669–10724, 2012

Jacobson, A. R., Fletcher, S. E. M., Gruber, N., Sarmiento, J. L., and Gloor, M.: A joint atmosphere-ocean inversion for surface fluxes of carbon dioxide: 2. Regional results, Global Biogeochem. Cy., 21, GB1019, doi:10.1029/2005GB002556, 2007.

Kalnay, E., Kanamitsu, M., Kistler, R., Collins, W., Deaven, D., Gandin, L., Redell, M., Saha, S., White, G., Woollen, J., Zhu, Y., Chelliah, M., Ebisuzaki, W., Higgins, W., Janowiak, J., Mo, K. C., Ropelewski, C., Leetmaa, A., Reynolds, R., and Jenne, R.: The NCEP/NCAR Reanalysis Project, B. Am. Meteorol. Soc., 77, 437–471, 1996.

Kaltin, S., and Anderson, L. G.: Uptake of atmospheric carbon dioxide in Arctic shelf seas: evaluation of the relative importance of processes that influence pCO_2 in water transported over the Bering-Chukchi Sea shelf, Mar. Chem., 94, 67–79, 2005.

Keeling, C. D.: Surface ocean CO_2, in: The Global Carbon Cycle, edited by: Heimann, M., Springer Verlag, Heidelberg, 413–429, 1993.

Khatiwala, S., Primeau, F., and Hall, T.: Reconstruction of the history of anthropogenic CO_2 concentrations in the ocean, Nature, 462, 346–349, 2009.

Koffi, U., Lefevre, N., Kouadio, G., and Boutin, J.: Surface CO_2 parameters and air-sea CO_2 flux distribution in the Eastern equatorial Atlantic Ocean, J. Mar. Syst., 82, 135–144, 2010.

Le Quéré, C., Orr, J. C., Monfray, P., Aumont, O., and Madec, G.: Interannual variability of the oceanic sink of CO_2 from 1979 through 1997, Global Biogeochem. Cy., 14, 1247–1265, 2000.

Le Quéré, C., Rödenbeck, C., Buitenhuis, E. T., Conway, T. J., Langenfelds, R., Gomez, A., Labuschagne, C., Ramonet, M., Nakazawa, T., Metzl, N., Gillett, N., and Heimann, M.: Saturation of the Southern Ocean CO_2 sink due to recent climate change, Science, 316, 1735–1738, 2007.

Le Quéré, C., Raupach, M. R., Canadell, J. G., Marland, G., Bopp, L., Ciais, P., Conway, T. J., Doney, S. C., Feely, R. A., Foster, P., Friedlingstein, P., Gurney, K., Houghton, R. A., House, J. I., Huntingford, C., Levy, P. E., Lomas, M. R., Majkut, J., Metzl, N., Ometto, J. P., Peters, G. P., Prentice, I. C., Randerson, J. T., Running, S. W., Sarmiento, J. L., Schuster, U., Sitch, S., Takahashi, T., Viovy, N., van der Werf, G. R., and Woodward, F. I.: Trends in the sources and sinks of carbon dioxide, Nat. Geosci., 2, 831–836, 2009.

Le Quéré, C., Takahashi, T., Buitenhuis, E. T., Rödenbeck, C., and Sutherland, S. C.: Impact of climate change and variability on the global oceanic sink of CO_2, Global Biogeochem. Cy., 24, GB4007, doi:10.1029/2009GB003599, 2010.

BGD
9, 10669–10724, 2012

Lee, K., Tong, L. T., Millero, F. J., Sabine, C. L., Dickson, A. G., Goyet, C., Park, G. H., Wanninkhof, R., Feely, R. A., and Key, R. M.: Global relationships of total alkalinity with salinity and temperature in surface waters of the world's oceans, Geophys. Res. Lett., 33, L19605, doi:10.1029/2006GL027207, 2006.

Lefevre, N., Watson, A. J., Olsen, A., Ríos, A. F., Pérez, F. F., and Johannessen, T.: A decrease in the sink for atmospheric CO_2 in the North Atlantic, Geophys. Res. Lett., 31, L07306, doi:10.1029/2003GL018957, 2004.

Lenton, A. and Matear, R. J.: Role of the Southern Annular Mode (SAM) in Southern Ocean CO_2 uptake, Global Biogeochem. Cy., 21, GB2016, doi:10.1029/2006GB002714, 2007.

Levine, N. M., Doney, S. C., Lima, I., Wanninkhof, R., Bates, N. R., and Feely, R. A.: The impact of the North Atlantic Oscillation on the uptake and accumulation of anthropogenic CO_2 by the North Atlantic Ocean mode waters, Global Biogeochem. Cy., 25, GB3022, doi:10.1029/2010GB003892, 2011.

Lewis, E. and Wallace, D. W. R.: Program Development for CO_2 System Calculations, Carbon Dioxide Information Analysis Center, Oak Ridge National Laboratory, US Department of Energy, Oak Ridge, Tennessee, ORNL/DCIAC-105, 26, 1998.

Lovenduski, N. S., Gruber, N., and Doney, S. C.: Toward a mechanistic understanding of the decadal trends in the Southern Ocean carbon sink, Global Biogeochem. Cy., 22, GB3016, doi:10.1029/2007GB003139, 2008.

Manizza, M., Follows, M. J., Dutkiewicz, S., Menemenlis, D., McClelland, J. W., Hill, C. N., Peterson, B. J., and Key, R. M.: A model of the Arctic Ocean carbon cycle, J. Geophys. Res., 116, C12020, doi:10.1029/2011JC006998, 2011.

Marshall, J., Kushnir, Y., Battisti, D., Chang, P., Czaja, A., Dickson, R., Hurrell, J., McCartney, M., Saravanan, R., and Visbeck, M.: North Atlantic climate variability: phenomena, impacts and mechanism, Int. J. Climatol., 21, 1863–1898, 2001.

McGuire, A. D., Hayes, D. J., Kicklighter, D. W., Manizza, M., Zhuang, Q., Chen, M., Follows, M. J., Gurney, K. R., McCelland, J. W., Melillo, J. M., Peterson, B. J., and Prinn, R. G.: An analysis of the carbon balance of the Arctic Basin from 1997 to 2006, Tellus B, 62, 455–474, doi:10.1111/j.1600-0889.2010.00497.x, 2010.

McKinley, G., Follows, M. J., and Marshall, J.: Mechanisms of air-sea CO_2 flux variability in the equatorial Pacific and the North Atlantic, Global Biogeochem. Cy., 18, GB2011, doi:10.1029/2003GB002179, 2004a.

BGD
9, 10669–10724, 2012

McKinley, G. A., Rödenbeck, C., Gloor, M., Houweling, S., and Heimann, M.: Pacific dominance to global air-sea CO_2 flux variability: a novel atmospheric invesion agrees with ocean models, Geophys. Res. Lett., 31, L22308, doi:10.1029/2004GL021069, 2004b.

McKinley, G. A., Fay, A. R., Takahashi, T., and Metzl, N.: Convergence of atmsopheric and North Atlantic carbon dioxide trends on mutidecadal timescales, Nat. Geosci., 4, 606–610, doi:10.1038/NGEO1193, 2011.

Mehrbach, C., Culberson, C. H., Hawley, J. E., and Pytkowicz, R. M.: Measurement of the apparent dissociation constants of carbonic acid in seawater at atmospheric pressure, Limnol. Oceanogr., 18, 897–907, 1973.

Metzl, N., Corbière, A., Reverdin, G., Lenton, A., Takahashi, T., Olsen, A., Johannessen, T., Pierrot, D., Wanninkhof, R., Ólafsdóttir, S. R., Olafsson, J., and Ramonet, M.: Recent acceleration of the sea surface fCO_2 growth rate in the North Atlantic subpolar gyre (1993–2008) revealed by winter observations, Global Biogeochem. Cy., 24, GB4004, doi:10.1029/2009gb003658, 2010.

Mikaloff Fletcher, S. E., Gruber, N., Jacobson, A. R., Doney, S. C., Dutkiewicz, S., Gerber, M., Follows, M., Joos, F., Lindsay, K., Menemenlis, D., Mouchet, A., Müller, S. A., and Sarmiento, J. L.: Inverse estimates of anthropogenic CO_2 uptake, transport, and storage by the ocean, Global Biogeochem. Cy., 20, GB2002, doi:10.1029/2005GB002530, 2006.

Olsen, A., Omar, A. M., Bellerby, R. G. J., Johannessen, T., Ninnemann, U., Brown, K. R., Olsson, K. A., Olafsson, J., Nondal, G., Kivimae, C., Kringstad, S., Neill, C., and Olafsdottir, S.: Magnitude and origin of the anthropogenic CO_2 increase and ^{13}C Suess effect in the Nordic seas since 1981, Global Biogeochem. Cy., 20, GB3027, doi:10.1029/2005GB002669, 2006.

Olsen, A., Brown, K. R., Chierici, M., Johannessen, T., and Neill, C.: Sea-surface CO_2 fugacity in the subpolar North Atlantic, Biogeosciences, 5, 535–547, doi:10.5194/bg-5-535-2008, 2008.

Omar, A. M. and Olsen, A.: Reconstructing the time history of the air-sea CO_2 disequilibrium and its rate of change in the Eastern Subpolar North Atlantic, 1972–1989, Geophys. Res. Lett., 33, L04602, doi:10.1029/2005GL025425, 2006.

Omar, A. M., Johannessen, T., Olsen, A., Kaltin, S., and Rey, F.: Seasonal and interannual variability of the air-sea CO_2 flux in the Atlantic sector of the Barents Sea, Mar. Chem., 104, 203–213, 2007.

Oschlies, A.: NAO-induced long-term changes in nutrient supply to the surface waters of the North Atlantic, Geophys. Res. Lett., 28, 1751–1754, doi:10.1029/2000GL012328, 2001.

BGD
9, 10669–10724, 2012

Oudot, C., Ternon, J. F., and Lecomte, J.: Measurements of atmospheric and oceanic CO_2 in the Tropical Atlantic – 10 year after the 1982–1984 focal cruises, Tellus B, 47, 70–85, 1995.
Pabi, S., van Djiken, G. L., and Arrigo, K. R.: Primary production in the Arctic Ocean, 1998–2006, J. Geophys. Res., 113, C08005, doi:10.1029/2007JC004578, 2008.
Padin, X. A., Vázquez-Rodríguez, M., Castaño, M., Velo, A., Alonso-Pérez, F., Gago, J., Gilcoto, M., Álvarez, M., Pardo, P. C., de la Paz, M., Ríos, A. F., and Pérez, F. F.: Air-Sea CO_2 fluxes in the Atlantic as measured during boreal spring and autumn, Biogeosciences, 7, 1587–1606, doi:10.5194/bg-7-1587-2010, 2010.
Parard, G., Lefevre, N., and Boutin, J.: Sea water fugacity of CO_2 at the PIRATA mooring at 6° S, 10° W, Tellus B, 62, 636–648, 2010.
Peylin, P., Bousquet, P., Le Quéré, C., Sitch, S., Friedlingstein, P., McKinley, G., Gruber, N., Rayner, P., and Ciais, P.: Multiple constraints on regional CO_2 flux variations over land and oceans, Global Biogeochem. Cy., 19, GB1011, doi:10.1029/2003GB002214, 2005.
Pfeil, B., Olsen, A., Bakker, D. C. E., Hankin, S., Koyuk, H., Kozyr, A., Malczyk, J., Manke, A., Metzl, N., Sabine, C. L., Akl, J., Alin, S. R., Bellerby, R. G. J., Borges, A., Boutin, J., Brown, P. J., Cai, W.-J., Chavez, F. P., Chen, A., Cosca, C., Fassbender, A. J., Feely, R. A., González-Dávila, M., Goyet, C., Hardman-Mountford, N., Heinze, C., Hood, M., Hoppema, M., Hunt, C. W., Hydes, D., Ishii, M., Johannessen, T., Jones, S. D., Key, R. M., Körtzinger, A., Landschützer, P., Lauvset, S. K., Lefèvre, N., Lenton, A., Lourantou, A., Merlivat, L., Midorikawa, T., Mintrop, L., Miyazaki, C., Murata, A., Nakadate, A., Nakano, Y., Nakaoka, S., Nojiri, Y., Omar, A. M., Padin, X. A., Park, G.-H., Paterson, K., Perez, F. F., Pierrot, D., Poisson, A., Ríos, A. F., Salisbury, J., Santana-Casiano, J. M., Sarma, V. V. S. S., Schlitzer, R., Schneider, B., Schuster, U., Sieger, R., Skjelvan, I., Steinhoff, T., Suzuki, T., Takahashi, T., Tedesco, K., Telszewski, M., Thomas, H., Tilbrook, B., Tjiputra, J., Vandemark, D., Veness, T., Wanninkhof, R., Watson, A. J., Weiss, R., Wong, C. S., and Yoshikawa-Inoue, H.: A uniform, quality controlled, Surface Ocean CO_2 Atlas (SOCAT), submitted to Earth Syst. Sci. Data, 2012.
Philander, S. G. H.: Unusual conditions in the Tropical Atlantic Ocean in 1984, Nature, 322, 236–238, 1986.
Rachold, V., Lantuit, H., and Pollard, W.: Arctic Coastal Dynamics, Report of the 5th International Workshop, McGill University, Montreal, Canada, 131 pp., 2004.
Rayner, N. A., Parker, D. E., Horton, E. B., Folland, C. K., Alexander, L. V., Rowell, D. P., Kent, E. C., and Kaplan, A.: Global analyses of sea surface temperature, sea ice, and

BGD
9, 10669–10724, 2012

night marine air temperature since the late nineteenth century, J. Geophys. Res., 108, 4407, doi:10.1029/2002JD002670, 2003.

Rödenbeck, C.: Estimating CO_2 Sources and Sinks from Atmospheric Mixing Ratio Measurements Using a Global Inversion of Atmsopheric Transport, Max-Planck Institut fur Biogeochemie, Jena, 53 pp., 2005.

Rödenbeck, C., Keeling, R. F., Bakker, D. C. E., Metzl, N., Olsen, A., Sabine, C., and Heimann, M.: Sea-air CO_2 flux estimated from SOCAT surface-ocean CO_2 partial pressure data and atmospheric CO_2 mixing ratio data, Ocean Sci. Discuss., 9, 2273–2326, doi:10.5194/osd-9-2273-2012, 2012. 2012.

Sabine, C., Hankin, S., Koyuk, H., Bakker, D. C. E., Pfeil, B., Olsen, A., Metzl, N., Kozyr, A., Fassbender, A., Manke, A., Malczyk, J., Akl, J., Alin, S. R., Bellerby, R. G. J., Borges, A., Boutin, J., Brown, P. J., Cai, W.-J., Chavez, F. P., Chen, A., Cosca, C., Feely, R. A., González-Dávila, M., Goyet, C., Hardman-Mountford, N., Heinze, C., Hoppema, M., Hunt, C. W., Hydes, D., Ishii, M., Johannessen, T., Key, R. M., Körtzinger, A., Landschützer, P., Lauvset, S. K., Lefevre, N., Lenton, A., Lourantou, A., Merlivat, L., Midorikawa, T., Mintrop, L., Miyazaki, C., Murata, A., Nakadate, A., Nakano, Y., Nakaoka, S., Nojiri, Y., Omar, A. M., Padin, X. A., Park, G.-H., Paterson, K., Perez, F. F., Pierrot, D., Poisson, A., Rios, A. F., Salisbury, J., Santana-Casiano, J. M., Sarma, V. V. S. S., Schlitzer, R., Schneider, B., Schuster, U., Sieger, R., Skjelvan, I., Steinhoff, T., Suzuki, T., Takahashi, T., Tedesco, K., Telszewski, M., Thomas, H., Tilbrook, B., Vandemark, D., Veness, T., Watson, A. J., Weiss, R., Wong, C. S., and Yoshikawa-Inoue, H.: Surface Ocean CO_2 Atlas (SOCAT) gridded data products, submitted to Earth Syst. Sci. Data, 2012.

Sabine, C. L., Feely, R. A., Gruber, N., Key, R. M., Lee, K., Bullister, J. L., Wanninkhof, R., Wong, C. S., Wallace, D. W. R., Tilbrook, B., Millero, F. J., Peng, T. H., Kozyr, A., Ono, T., and Rios, A. F.: The oceanic sink for anthropogenic CO_2, Science, 305, 367–371, 2004.

Santana-Casiano, J. M. and González-Dávila, M.: Carbon dioxide fluxes in the Benguela upwelling system during winter and spring. A comparison between 2005 and 2006, Deep-Sea Res. II, 56, 533–541, 2009.

Santana-Casiano, J. M., González-Dávila, M., Rueda, M. J., Llinas, O., and Gonzalez-Davila, E. F.: The interannual variability of oceanic CO_2 parameters in the Northeast Atlantic subtropical gyre at the ESTOC site, Global Biogeochem. Cy., 21, GB1015, doi:10.1029/2006GB002788, 2007.

BGD
9, 10669–10724, 2012

Sarmiento, J. L. and Le Quéré, C.: Oceanic carbon dioxide uptake in a model of century-scale global warming, Science, 274, 1346–1350, 1996.

Sarmiento, J. L., Slater, R., Barber, R., Bopp, L., Doney, S. C., Hirst, A. C., Kleypas, J., Matear, R., Mikolajewicz, U., Monfray, P., Soldatov, V., Spall, S. A., and Stouffer, R.: Response of ocean ecosystems to climate warming, Global Biogeochem. Cy., 18, GB3003, doi:10.1029/2003GB002134, 2004.

Schuster, U. and Watson, A. J.: A variable and decreasing sink for atmospheric CO_2 in the North Atlantic, J. Geophys. Res., 112, C11006, doi:10.1029/2006JC003941, 2007.

Schuster, U., Watson, A. J., Bates, N., Corbière, A., González-Dávila, M., Metzl, N., Pierrot, D., and Santana-Casiano, J. M.: Trends in North Atlantic sea surface pCO_2 from 1990 to 2006, Deep-Sea Res. II, 56, 620–629, 2009.

Sweeney, C., Gloor, E., Jacobson, A. R., Key, R. M., McKinley, G., Sarmiento, J. L., and Wanninkhof, R.: Constraining global air-sea gas exchange for CO_2 with recent bomb ^{14}C measurements, Global Biogeochem. Cy., 21, GB2015, doi:10.1029/2006GB002784, 2007.

Takahashi, T., Sutherland, S. C., Sweeney, C., Poisson, A., Metzl, N., Tilbrook, B., Bates, N., Wanninkhof, R., Feely, R. A., Sabine, C., Olafsson, J., and Nojiri, Y.: Global sea-air CO_2 flux based on climatological surface ocean pCO_2, and seasonal biological and temperature effects, Deep-Sea Res. Pt. II, 49, 1601–1622, 2002.

Takahashi, T., Sutherland, S. C., Wanninkhof, R., Sweeney, C., Feely, R. A., Chipman, D. W., Hales, B., Friederich, G., Chavez, F., Sabine, C., Watson, A. J., Bakker, D. C., Schuster, U., Metzl, N., Yoshikawa-Inoue, H., Ishii, M., Midorikawa, T., Nojiri, Y., Körtzinger, A., Steinhoff, T., Hoppema, M., Olafsson, J., Arnarson, T. S., Tilbrook, B., Johannessen, T., Olsen, A., Bellerby, R., Wong, C. S., Delille, B., Bates, N. R., and De Baar, H. J. W.: Climatological mean and decadal change in surface ocean pCO_2, and net sea-air CO_2 flux over the global oceans, Deep-Sea Res. Pt. II, 56, 554–577, 2009.

Thomas, H., Prowe, A. E. F., Lima, I. D., Doney, S. C., Wanninkhof, R., Greatbatch, R. J., Schuster, U., and Corbiére, A.: Changes in the North Atlantic Oscillation influence CO_2 uptake in the North Atlantic over the past 2 decades, Global Biogeochem. Cy., 22, GB4027, doi:10.1029/2007GB003167, 2008.

Ullman, D. J., McKinley, G. A., Bennington, V., and Dutkiewicz, S.: Trends in the North Atlantic carbon sink: 1992–2006, Global Biogeochem. Cy., 23, GB4011, doi:10.1029/2008GB003383, 2009.

BGD
9, 10669–10724, 2012

Wanninkhof, R.: Relationship between wind speed and gas exchange over the ocean, J. Geophys. Res., 97, 7373–7382, 1992.
Wanninkhof, R., Park, G. H., Takahash.T, Sweeney, C., Feely, R., Nojiri, Y., Gruber, N., Doney, S., et al.: Global Ocean Carbon Uptake: Magnitude, Variability and Trends, submitted to Biogeosciences, 2012.
Watson, A. J., Schuster, U., Bakker, D. C. E., Bates, N. R., Corbière, A., González-Dávila, M., Friedrich, T., Hauck, J., Heinze, C., Johannessen, T., Körtzinger, A., Metzl, N., Olafsson, J., Olsen, A., Oschlies, A., Padin, X. A., Pfeil, B., Santana-Casiano, J. M., Steinhoff, T., Telszewski, M., Rios, A. F., Wallace, D. W. R., and Wanninkhof, R.: Tracking the Variable North Atlantic Sink for Atmospheric CO_2, Science, 326, 1391–1393, 2009.
Weiss, R. F.: Carbon dioxide in water and seawater: the solubility of a non-ideal gas, Mar. Chem., 2, 203–215, 1974.
Zhang, J., Spitz, Y. H., Steele, M., Ashjian, C., Campbell, R., Berline, L., and Matrai, P.: Modeling the impact of declining sea ice on the Arctic marine planktonic ecosystem, J. Geophys. Res., 115, C10015, doi:10.1029/2009JC005387, 2010.

BGD
9, 10669–10724, 2012

Table 1. RECCAP atmospheric inversions included in this study.

Model abbreviation	Years
LSCE_an_v2.1	1996–2004
LSCE_var_v1.0	1990–2008
C13_CCAM	1992–2008
C13_MATCH	1992–2008
CTracker_US	2001–2008
CTracker_EU	2001–2008
JENA_s96_v3.3	1996–2009
RIGC_Patra	1993–2006
JMA_2010	1990–2008
TRCOM_mean	1995–2008
NICAM_NIWA	1990–2007

BGD
9, 10669–10724, 2012

Table 2. Details of the ocean biogeochemical models included in this study.

Model abbreviation	Model	Reference	Years
BER	MICOM-HAMOCC	Assmann et al. (2010)	1990 to 2009
CSI	CSIRO	Lenton and Matear (2007)	1959 to 2009
BEC	CCSM-BEC	Thomas et al. (2008)	1990 to 2009
ETHk15	CCSM-ETH	Graven et al. (2012)	1990 to 2007
LSCE	NEMO-PISCES	Aumont and Bopp (2006)	1990 to 2009
UEAncep	NEMO-PlankTOM5 NCEP	Le Quéré et al. (2007)	1990 to 2009

BGD
9, 10669–10724, 2012

Table 3. Latitudinal boundaries of sub-regions in the Arctic and Atlantic.

Basin	Latitude boundaries	Longitudinal boundaries	Area (10^{12} m^2)
Arctic	76° N to 90° N	excl. Baffin Bay and Nordic Seas (SW of 76° N, 19° E)	9.61
North Subpolar	49° N to 76° N	West of 19° E	8.63
North Subtropics	18° N to 49° N		23.68
Equatorial	18° S to 18° N		23.49
South Subtropics	44° S to 18° S	West of 19° E	18.44
Total			83.84

BGD
9, 10669–10724, 2012

Table 4. 1990 to 2009 mean flux in each region and whole Arctic/Atlantic for Tier 1 methodologies (climatology, ocean inversion, atmospheric inversion, and ocean biogeochemical models), and observations (SOCAT MPR and pCO_2 database). Pixel areas for each region are given in the last column of Table 3. Atmospheric inversions begin in 1995. The best estimate for each region except the Arctic is the mean of the pCO_2 climatology and Ocean Inversion, with uncertainty from standard error propagation. The Arctic best estimate is derived from other studies, as explained in the text. Uncertainty of the best estimate for the whole Arctic+Atlantic is calculated with standard error propagation.

	pCO_2 climatology		Ocean inversion		Atmospheric inversions		Ocean biogeochemical models		SOCAT MPR		pCO_2 database		Best estimate
	Pg C yr^{-1}	mol m^{-2} yr^{-1}	**Pg C yr^{-1}**	mol m^{-2} yr^{-1}	**Pg C yr^{-1}**	mol m^{-2} yr^{-1}	**Pg C yr^{-1}**	mol m^{-2} yr^{-1}	**Pg C yr^{-1}**	mol m^{-2} yr^{-1}	**Pg C yr^{-1}**	mol m^{-2} yr^{-1}	**Pg C yr^{-1}**
Arctic	**−0.03 ±0.02**	−0.28 ±0.14	**0.00 ±0.04**	0.02 ±0.35	**−0.04 ±0.02**	−0.37 ±0.15	**−0.05 ±0.03**	−0.41 ±0.23					**−0.12 ±0.06**
North Subpolar	**−0.23 ±0.12**	−2.2 ±1.1	**−0.19 ±0.06**	−1.8 ±0.53	**−0.28 ±0.03**	−2.7 ±0.28	**−0.17 ±0.02**	−1.62 ±0.22	**−0.07 ±0.04**	−0.71 ±0.36	**−0.30 ±0.13**	−2.9 ±1.3	**−0.21 ±0.06**
North Subtropics	**−0.19 ±0.09**	−0.66 ±0.33	**−0.34 ±0.08**	−1.2 ±0.29	**−0.31 ±0.03**	−1.1 ±0.43	**−0.13 ±0.03**	−0.46 ±0.07	**−0.18 ±0.09**	−0.62 ±0.31	**−0.24 ±0.16**	−0.85 ±0.56	**−0.26 ±0.06**
Equatorial	**0.11 ±0.05**	0.39 ±0.19	**0.13 ±0.06**	0.45 ±0.21	**0.12 ±0.05**	0.44 ±0.21	**0.15 ±0.06**	0.51 ±0.20	**0.10 ±0.05**	0.34 ±0.17	**0.12 ±0.14**	0.43 ±0.49	**0.12 ±0.04**
South Subtropics	**−0.10 ±0.05**	−0.46 ±0.23	**−0.17 ±0.05**	−0.78 ±0.25	**−0.13 ±0.02**	−0.57 ±0.10	**−0.17 ±0.01**	−0.76 ±0.04	**−0.25 ±0.12**	−1.1 ±0.56	**−0.21 ±0.23**	−0.96 ±1.0	**−0.14 ±0.04**
Arctic + Atlantic	**−0.45 ±0.17**	−0.44 ±0.17	**−0.56 ±0.13**	−0.56 ±0.13	**−0.64 ±0.07**	−0.64 ±0.07	**−0.37 ±0.07**	−0.37 ±0.07	**−0.40 ±0.16**	−0.45 ±0.18	**−0.63 ±0.34**	−0.71 ±0.38	**−0.61 ±0.12**

BGD
9, 10669–10724, 2012

Table 5. Correlations of seasonal cycle for each region and each methodology. Significant correlations ($p < 0.05$) are in bold.

	pCO_2 climatology	Atmospheric Inversions	Ocean Models	SOCAT MPR	pCO_2 database
(a) Arctic					
pCO_2 climatology	1	**0.70**	**0.68**		
Atm. Inversions		1	0.17		
Ocean models			1		
(b) North Subpolar					
pCO_2 climatology	1	−0.31	**0.69**	−0.36	−0.31
Atm. Inversions		1	**−0.81**	−0.38	−0.22
Ocean models			1	**−0.59**	0.04
SOCAT MPR				1	0.56
(c) North Subtropics					
pCO_2 climatology	1	**0.94**	**1.0**	**0.97**	**0.96**
Atm. Inversions		1	**0.96**	**0.97**	**0.96**
Ocean models			1	**0.99**	**0.98**
SOCAT MPR				1	**1.0**
(d) Equatorial					
pCO_2 climatology	1	−0.04	−0.04	0.23	0.14
Atm. Inversions		1	−0.10	0.44	0.05
Ocean models			1	0.27	**0.88**
SOCAT MPR				1	0.18
(e) South Subtropics					
pCO_2 climatology	1	**0.90**	**0.85**	**0.84**	**0.85**
Atm. Inversions		1	**0.84**	**0.90**	**0.93**
Ocean models			1	**0.97**	**0.95**
SOCAT MPR				1	**0.99**

BGD
9, 10669–10724, 2012

Table 6. Standard deviation of low frequency IAV for each region and each methodology in units (Pg C yr^{-1}). Results were deseasonalized and detrended before the calculation of the standard deviation.

	Standard Deviation (Pg C yr^{-1})			
	Atmospheric inversions	Ocean biogeochemical models	SOCAT MPR	pCO_2 database
Time periods	1995–2009	1990–2009	1997 to 2007	1990–2009
Arctic	0.003	0.005		
North Subpolar	0.008	0.008	0.004	0.016
North Subtropics	0.026	0.016	0.008	0.015
Equatorial	0.023	0.014	0.004	0.009
South Subtropics	0.026	0.011	0.008	0.012
Arctic + Atlantic	0.055	0.029	0.015	0.046

BGD
9, 10669–10724, 2012

Table 7. Correlations of low frequency interannual variability for each region between methodologies. Correlation to the monthly NAO index, smoothed with a 12-month filter, are included for all regions. For the North Subtropics, we include correlations to BATS and ESTOC. All correlations are at zero time lag. Significant correlations ($p < 0.05$) are in bold. Time periods for each methodology are as noted in Table 6.

	Atm. inversions	Ocean models	SOCAT MPR	pCO_2 database	NAO	BATS	ESTOC
(a) Arctic							
Atm. inversions	1	0.07			**0.24**		
Ocean models		1			−0.09		
(b) North Subpolar							
Atm. inversions	1	−0.02	**0.26**	**0.20**	−0.01		
Ocean models		1	−0.10	**0.32**	**−0.20**		
SOCAT MPR			1	**0.89**	0.06		
pCO_2 database				1	**0.15**		
(c) North Subtropics							
Atm. inversions	1	**0.20**	−0.13	**0.23**	−0.05	**0.26**	−0.10
Ocean models		1	0.14	**0.49**	**0.14**	**0.30**	−0.06
SOCAT MPR			1	0.08	0.02	**0.35**	**0.20**
pCO_2 database				1	**0.20**	**0.49**	0.11
NAO					1	**0.17**	−0.35
BATS						1	**0.26**
(d) Equatorial							
Atm. inversions	1	**0.40**	**0.39**	**−0.39**	**−0.51**		
Ocean models		1	**0.72**	0.13	**−0.43**		
SOCAT MPR			1	0.06	0.11		
pCO_2 database				1	**0.35**		
(e) South Subtropics							
Atm. inversions	1	**0.56**	**−0.50**	**−0.31**	0.02		
Ocean models		1	0.15	**0.55**	**0.40**		
SOCAT MPR			1	**0.97**	**0.30**		
pCO_2 database				1	**0.36**		
(f) Arctic + Atlantic							
Atm. inversions	1	**0.32**	−0.07	**−0.15**	**−0.25**		
Ocean models		1	**0.55**	**0.54**	−0.05		
SOCAT MPR			1	**0.87**	**0.28**		
pCO_2 database				1	**0.29**		

BGD
9, 10669–10724, 2012

Table 8. Linear trends of the spatially integrated sea-air CO_2 flux for each region and whole Arctic/Atlantic, 1995 to 2009 ($Tg\,C\,yr^{-1}\,decade^{-1}$) for the atmospheric inversions, the ocean biogeochemical models and the pCO_2 database. Trends are a linear fit to the low frequency median flux IAV (i.e. Fig. 6), with 2σ confidence. Trends distinguishable from zero are indicated in bold.

	Atm. inversions	Ocean biogeochemical models	pCO_2 database
Arctic	**–2.4 ± 1.5**	**–9.0 ± 1.6**	
North Subpolar	–3.1 ± 3.9	**–4.2 ± 3.6**	**–75 ± 3.4**
North Subtropics	**–33 ± 12**	**–19 ± 7.7**	**–53 ± 3.3**
Equatorial	**33 ± 11**	–4.7 ± 6.6	**–35 ± 2.1**
South Subtropics	**23 ± 13**	–3.5 ± 3.5	**–120 ± 3.2**
Arctic + Atlantic	17 ± 26	**–34 ± 14**	**–290 ± 7.4**

BGD
9, 10669–10724, 2012

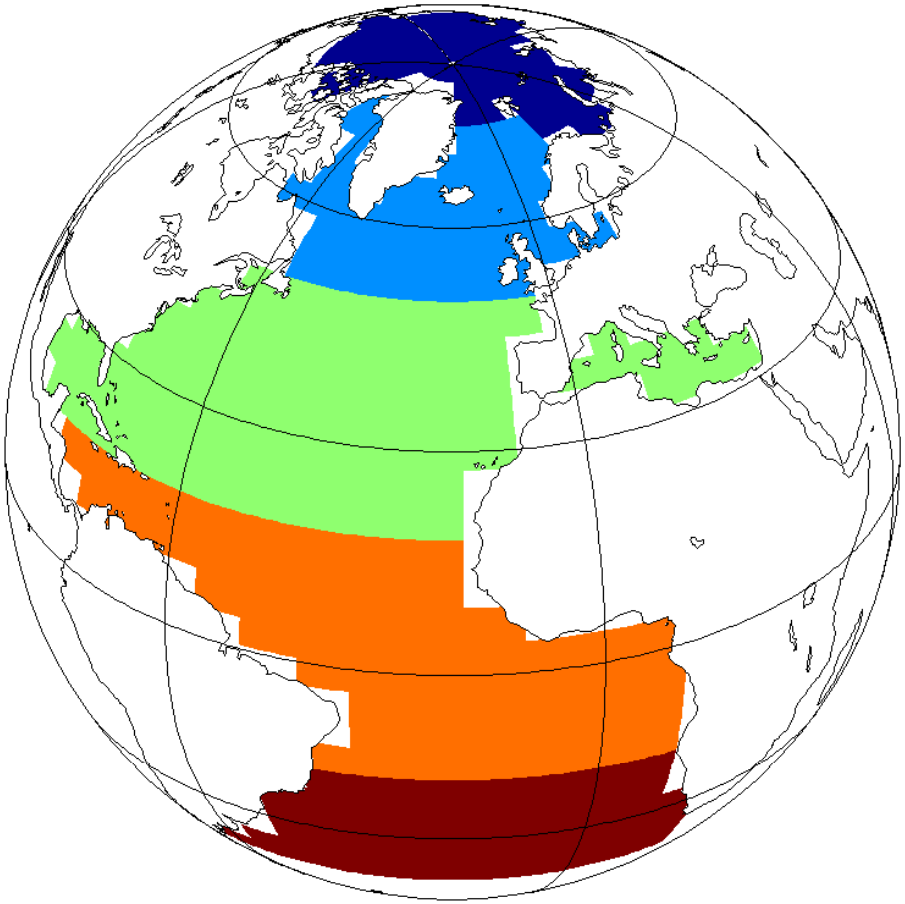

Fig. 1. The 5 RECCAP regions in the Arctic and Atlantic basins.

BGD
9, 10669–10724, 2012

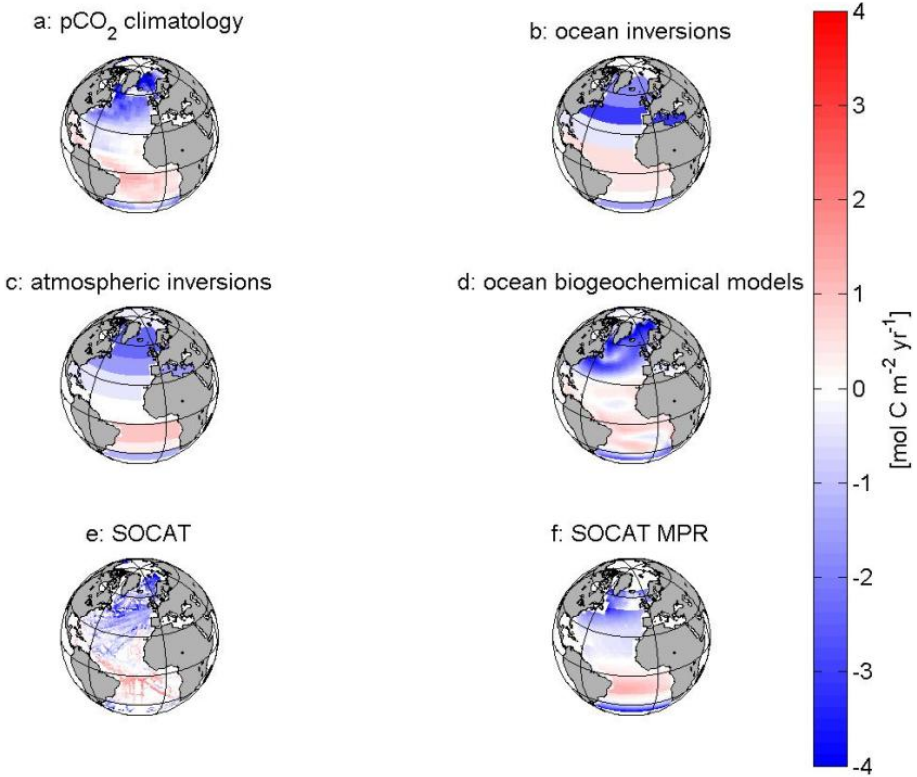

Fig. 2. Long-term temporal mean of the sea-air flux of CO_2 ($mol\,m^{-2}\,yr^{-1}$) of Tier 1 methodologies: **(a)** the pCO_2 climatology of 2000, **(b)** the ocean inversion, **(c)** the median of 11 atmospheric inversions, **(d)** the median of 6 ocean biogeochemical models; additionally, we show the LTM of the SOCAT gridded product and the SOCAT MPR.

BGD
9, 10669–10724, 2012

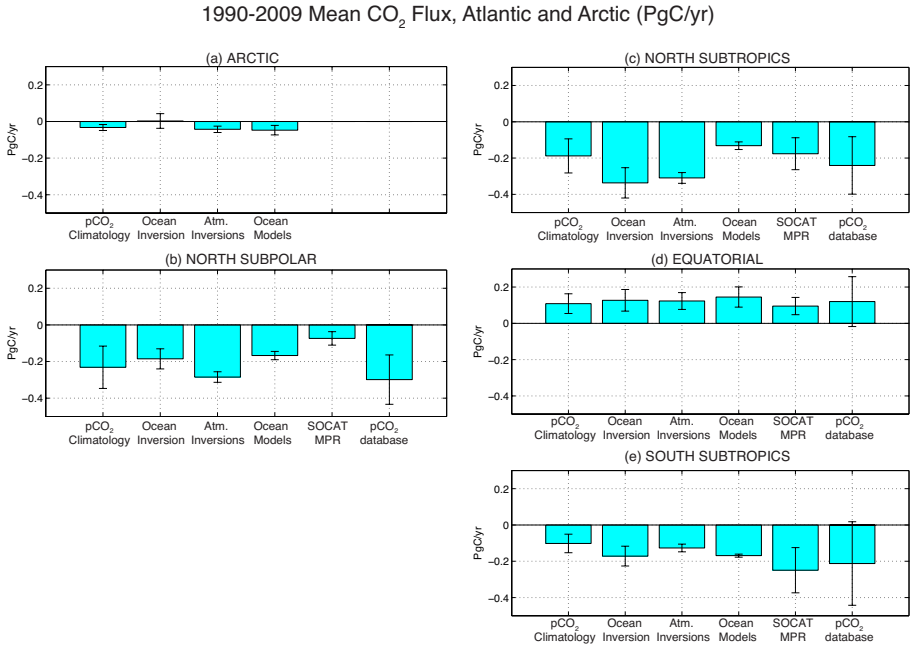

Fig. 3. The 1990–2009 long-term mean sea-air CO_2 flux (Pg C yr^{-1}) in the **(a)** Arctic, **(b)** North Subpolar, **(c)** North Subtropics, **(d)** Equatorial, and **(e)** South Subtropics for Tier 1 methodologies: pCO_2 climatology, median of ocean inversion, median of atmospheric inversions, median of ocean models, and additionally for SOCAT MPR and pCO_2 database IAV. Rivers fluxes of Jacobson et al. (2007) have been added to the ocean model estimates as required (described in text). Uncertainty is the median absolute deviation for the atmospheric inversions and ocean models, 50 % of the mean for the pCO_2 climatology and SOCAT MPR, the mean annual uncertainty for pCO_2 database trend, and the published uncertainty for the ocean inversion (Gruber et al., 2009).

BGD
9, 10669–10724, 2012

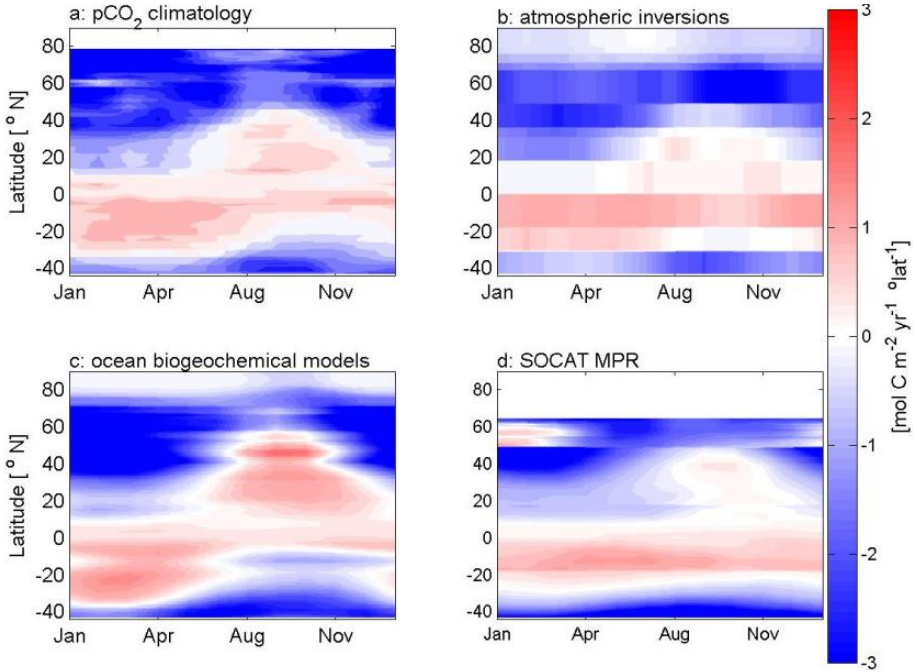

Fig. 4. Zonally averaged long-term mean seasonal cycle of Atlantic sea-to-air CO_2 flux density (mol C m^{-2} yr^{-1} per degree of latitude), based on the Tier 1 methodologies: **(a)** pCO_2 climatology, **(b)** atmospheric inversions' median, and **(c)** ocean biogeochemical models' median; additionally we show **(d)** the observations based SOCAT MPR. The pCO_2 database is not shown because it is not a gridded product.

BGD
9, 10669–10724, 2012

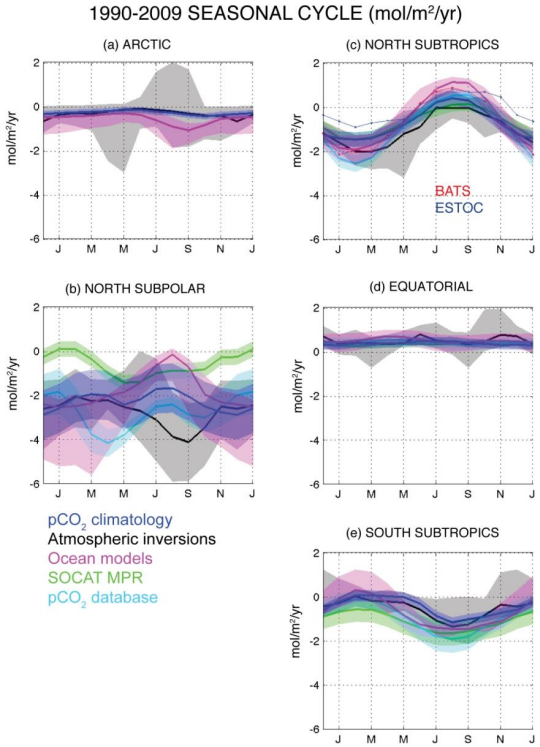

Fig. 5. Mean seasonal cycles of sea-air CO_2 flux density (mol m^{-2} yr^{-1}) the **(a)** Arctic, **(b)** North Subpolar, **(c)** North Subtropics, **(d)** Equatorial, and **(e)** South Subtropics for the pCO_2 climatology (light blue), atmospheric inversions (black), and ocean biogeochemical models (magenta), SOCAT MPR (yellow), pCO_2 database (cyan), and at the BATS and ESTOC sites in the North Subtropics (dark blue and red, respectively). Shading indicates the spread between max and min from the atmospheric inversions and ocean biogeochemical models, 50 % of the mean for the pCO_2 climatology and SOCAT, and the uncertainty of the harmonic fit for the pCO_2 database IAV. Means are in both space and for all years available for each methodology.

BGD
9, 10669–10724, 2012

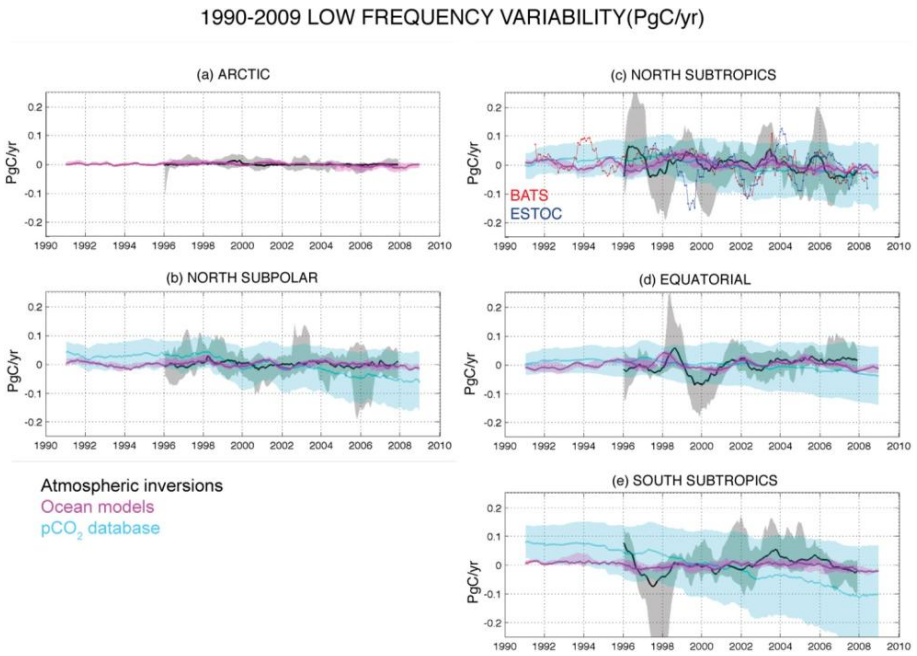

Fig. 6. Low frequency IAV of spatially integrated sea-air CO_2 fluxes (Pg C yr^{-1}) in the **(a)** Arctic, **(b)** North Subpolar, **(c)** North Subtropics, **(d)** Equatorial, and **(e)** South Subtropics for atmospheric inversions (black), ocean models (magenta), SOCAT MPR (yellow) and pCO_2 database (cyan). Shaded region is the spread between max and min from the atmospheric inversions and ocean models, and the uncertainty of the harmonic fit for the pCO_2 database. SOCAT MPR is not included because its time scale is too short.

BGD
9, 10669–10724, 2012